 CMES, vol.92, no.4, pp.387-421, 2013

Flexural wave dispersion in finitely pre-strained solid and hollow circular cylinders made of compressible materials

S. D. Akbarov [1,2]

Abstract: Flexural wave dispersion in finitely pre-stretched (or pre-compressed) solid and hollow, circular cylinders is investigated with the use of the three-dimensional linearized theory of elastic waves in initially stressed bodies. It is assumed that the initial strains in the cylinders are homogeneous and correspond to the uniaxial tension, or compression, along their central axes. The elasticity relations of the cylinders' materials are described by the harmonic potential. The analytical solution of the corresponding field equations is presented and, using these solutions, the dispersion equations for the cases under consideration are obtained. The dispersion equations are solved numerically and based on these solutions, dispersion curves and dispersion diagrams are constructed for various values of the elongation parameter through which the magnitude of the initial strains is determined. The numerical results are obtained for the first and second lowest modes of the solid cylinder and for the first three lowest modes of the hollow cylinder. According to the analyses, in particular, it is established that the finite initial uniaxial stretching, as well the finite initial uniaxial compressing, change the dispersion of the flexural waves in the solid and hollow cylinders not only quantitatively, but also qualitatively.

Keywords: Flexural wave dispersion, backward wave, anomalous dispersion, initial strain, cylinder

1 Introduction

Flexural waves are the most complicated waves which can propagate in infinite circular cylinders. Longitudinal and torsional axisymmetric waves in these cylinders are particular cases of flexural waves. At the same time, flexural waves are more

[1] Yildiz Technical University, Faculty of Mechanical Engineering, Department of Mechanical Engineering, Yildiz Campus, 34349, Besiktas, Istanbul-Turkey;
E-mail: akbarov@yildiz.edu.tr

[2] Institute of Mathematics and Mechanics of the National Academy of Sciences of Azerbaijan, 37041, Baku, Azerbaijan.

real than axisymmetric waves and can be generated by almost all types of time-harmonic non-axisymmetric distributed external time–harmonic dynamical forces acting on a certain part of the cylinder. Therefore, investigations of the propagation and dispersion laws of flexural waves have been the subject of many researchers, which have been made by employing both the three-dimensional exact equations of the linear theory of elastodynamics (see Hudson (1943), Pao and Mindlin (1960), Abramson (1957) and others) and the equation of motion for approximate beam and shell theories (see Cooper and Naghdi (1957) and others). A detailed review of earlier related works was given in a paper by Thurston (1978). Note that these investigations continue to this day especially with respect to the circular cylinders which are made of composite materials (see Yamakawa and Murakami (1997), Yuan and Hsieh (1998), Ilmenkov and Kleshchev (2012) and others).

It should be noted that the present state of the governing branches of modern industry such as civil engineering, mechanical engineering, shipbuilding, aircraft and others, requires the study of the influence of the nonlinear effects on the dispersion of the flexural waves in circular cylinders. One of the main sources, according to which these nonlinear effects arise, is the initial stresses in cylinders. It is evident that the problems related to the wave propagation in the initially stressed bodies cannot be investigated within the framework of field equations of the linear theory of elastodynamics. Therefore, the studies of these problems are made within the scope of the Three-Dimensional Linearized Theory of Elastic Waves in Initially Stressed Bodies (TLTEWISB).

The relations and equations of the TLTEWISB are obtained from the exact relations and equations of the non-linear theory of elastodynamics by linearization with respect to small dynamical perturbations. The general questions of the TLTEWISB have been elaborated in many investigations such as in works by Biot (1965), Truestell (1961), Eringen and Suhubi (1975), Guz (2004) and others. It should be noted that there are some versions of the TLTEWISB which were developed in the monograph by Guz (2004). These versions of the TLTEWISB are distinguished from each other with respect to the magnitude of the initial strains. The version of the TLTEWISB developed for high-elastic materials, according to which the initial strains in the bodies are determined within the scope of the nonlinear theory of elasticity without any restrictions on the magnitude of the initial strains, is called the large (or finite) initial deformation version. The version of the TLTEWISB, according to which the initial stress-strain state in bodies is determined within the scope of the geometrically non-linear theory of elasticity and under which changes to the elementary areas and volumes as a result of the initial deformation are not taken into account, is called the first version of the small initial deformation theory of the TLTEWISB. The second version has an initial stress-

strain state in bodies, which is determined within the scope of the classical linear theory of elasticity.

Now we consider a brief review of the investigations related to flexural wave propagation in a pre-stressed circular solid cylinder. One of the first attempts in this field was made by Mott (1973) in which, within the scope of the aforementioned second version of the small initial deformation theory of the TLTEWISB, the influence of the axial extensional as well as the axial compressional initial strains, on the phase velocity of the first fundamental mode of the flexural waves was studied. The material of the cylinder was assumed to be isotropic and in some particular cases (for the case where the cylinder is made of Aluminum) it was established that as a result of the existence of acceptable values of the initial extensional (compressional) axial stress, the phase velocity of the flexural waves can increase (decrease) about 15%.

In papers by Guz, Kushnir and Makhort (1975) and Kushnir (1983) within the scope of the aforementioned first version of the small initial deformation theory of the TLTEWISB, the flexural wave propagation in the initially axially strained solid (Guz, Kushnir and Makhort (1975)) and hollow (Kushnir (1983)) cylinders was studied. The mechanical relations of the cylinders' materials are described through the Murnaghan potential, as a result of which the influence of the third order elastic constants on the wave propagation velocity is also taken into account. Note that in these works numerical investigations were made for the first five modes only in the case where the initial stress in the cylinder, which is fabricated from steel, is a stretching one and as a result of these investigations it was established that the character of the influence of the initial stresses on the flexural wave propagation velocity depends significantly on the values of the wavenumber and the number of the mode.

Note that the results of the previous works are acceptable for cylinders made of comparatively rigid materials such as Aluminum and Steel, but not for cylinders made of high elastic materials with finite initial strains. The first attempt for the study of the longitudinal wave propagation in the finite pre-strained solid cylinder was made by Belward (1976) for the case where the cylinder is composed of an incompressible Mooney material. However, in the paper by Belward (1976) there are no numerical results nor any analyses related to the flexural waves.

To the best of the author's knowledge, up to now there has not been any investigation related to the study of flexural wave propagation in the initially finite pre-strained circular cylinders. However, learning the rules of flexural wave propagation in the finite pre-strained solid and hollow cylinders made of highly-elastic elastomers or polymers can be useful for more accurate and correct understanding and to control the dynamical processes occurring in these cylinders. Moreover, the study of flexural wave propagation and dispersion in finite pre-strained cylinders

can be taken as the first step of the study of more complicated problems on the dynamical processes related to the highly-elastic polymer tubes which are used for transportation of various kinds of fluids.

Thus, these and many other reasons necessitate the investigation of the flexural wave dispersion in the finite pre-strained solid and hollow cylinders made of highly-elastic compressible and incompressible materials. In the present work we make the first attempts in this field in the case where the cylinders are made from compressible highly-elastic materials and their mechanical relations are described by the harmonic potential. The investigations are made by utilizing the large (or finite) initial deformation version of the TLTEWISB and the numerical results on the influence of the initial strains on the magnitude and on the character of the flexural wave dispersions in the cylinders are presented and discussed for a few of the lowest modes.

Moreover, the investigations carried out in the current paper can also be considered as developments of the studies by the author and his students (see Akbarov and Guliev (2009, 2010), Akbarov and Ipek (2010, 2012), Akbarov, Guliev and Tekercioglu (2010), Akbarov, Guliev and Kepceler (2011), Akbarov, Kepceler and Egilmez (2011, 2012), Kepceler (2010) and Ozturk and Akbarov (2008, 2009a, 2009b) related to axisymmetric wave propagation in compound cylinders for the non-axisymmetric wave propagation case.

2 Formulation of the problem and governing field equations

We consider the solid (Fig. 1a) and hollow cylinders (Fig. 1b) and assume that the radius of the solid cylinder and the outer radius of the hollow cylinder is R, but the thickness of the latter is h. In the natural state we determine the position of the points of the cylinders by the Lagrangian coordinates in the cylindrical system of coordinates $Or\theta z$. Assume that in the initial state the cylinders are stretched or compressed statically along the Oz axis and as a result the axisymmetric homogeneous initial stress-strain state arises. The values related to the initial state we denote by the upper index "0" and suppose that the initial state is determined by the following displacement field:

$$u_r^0 = (\lambda_1 - 1)r, \quad u_\theta^0 = 0, \quad u_z^0 = (\lambda_3 - 1)r, \quad \lambda_1 \neq \lambda_3, \tag{1}$$

where u_r^0 (u_z^0) is the displacement, but $\lambda_1(\lambda_3)$ is the elongation parameter along the radial direction (along the Oz axis).

For the initial state of the cylinders, we associate the Lagrangian cylindrical system of coordinates $O'r'\theta'z'$ and introduce the following notation

$$r' = \lambda_1 r, \quad z' = \lambda_3 z \tag{2}$$

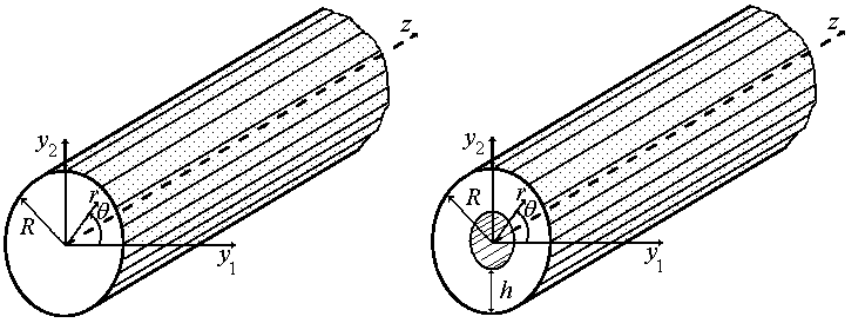

Figure 1: The geometry of the solid (a) and hollow (b) cylinders

The values related to the system of coordinates associated with the initial state below, i.e. with $O'r'\theta'z'$, will be denoted by an upper prime.

Within this framework, let us investigate the flexural wave propagation along the $O'z'$ axis in the cylinders using the coordinates r', θ' and z' in the framework of the TLTEWISB. Thus, we write the basic relations of the TLTEWISB for the case considered.

The equations of motion:

$$\frac{\partial Q'_{r'r'}}{\partial r'}+\frac{1}{r'}\frac{\partial Q'_{\theta'r'}}{\partial \theta'}+\frac{\partial Q'_{z'r'}}{\partial z'}+\frac{1}{r'}(Q'_{r'r'}-Q'_{\theta'\theta'})=\rho'\frac{\partial^2 u_{r'}}{\partial t^2},$$

$$\frac{\partial Q'_{r'\theta'}}{\partial r'}+\frac{1}{r'}\frac{\partial Q'_{\theta'\theta'}}{\partial \theta'}+\frac{\partial Q'_{z'\theta'}}{\partial z'}+\frac{1}{r'}(Q'_{r'\theta'}+Q'_{\theta'r'})=\rho'\frac{\partial^2 u_{\theta'}}{\partial t^2},$$

$$\frac{\partial Q'_{r'z'}}{\partial r'}+\frac{1}{r'}\frac{\partial Q'_{\theta'z'}}{\partial \theta'}+\frac{\partial Q'_{z'z'}}{\partial z'}+\frac{1}{r'}Q'_{r'z'}=\rho'\frac{\partial^2 u_{z'}}{\partial t^2}. \tag{3}$$

The elasticity relations:

$$Q'_{r'r'}=\omega'_{1111}\frac{\partial u_{r'}}{\partial r'}+\omega'_{1122}\frac{1}{r'}(\frac{\partial u_{\theta'}}{\partial \theta'}+u_{r'})+\omega'_{1133}\frac{\partial u_{z'}}{\partial z'},$$

$$Q'_{\theta'\theta'}=\omega'_{2211}\frac{\partial u_{r'}}{\partial r'}+\omega'_{2222}\frac{1}{r'}(\frac{\partial u_{\theta'}}{\partial \theta'}+u_{r'})+\omega'_{2233}\frac{\partial u_{z'}}{\partial z'},$$

$$Q'_{z'z'}=\omega'_{3311}\frac{\partial u_{r'}}{\partial r'}+\omega'_{3322}\frac{1}{r'}(\frac{\partial u_{\theta'}}{\partial \theta'}+u_{r'})+\omega'_{3333}\frac{\partial u_{z'}}{\partial z'},$$

$$Q'_{r'\theta'}=\omega'_{1221}\frac{\partial u_{\theta'}}{\partial r'}+\omega'_{1212}(\frac{1}{r'}\frac{\partial u_{r'}}{\partial \theta'}-\frac{1}{r'}u_{\theta'}),$$

$$Q'_{\theta'r'}=\omega'_{2121}\frac{\partial u_{\theta'}}{\partial r'}+\omega'_{2112}(\frac{1}{r'}\frac{\partial u_{r'}}{\partial \theta'}-\frac{1}{r'}u_{\theta'}),$$

$$Q'_{z'\theta'} = \omega'_{3223}\frac{\partial u_{\theta'}}{\partial z'} + \omega'_{3232}\frac{\partial u_{z'}}{r'\partial\theta'}, \quad Q'_{\theta'z'} = \omega'_{2323}\frac{\partial u_{\theta'}}{\partial z'} + \omega'_{2332}\frac{\partial u_{z'}}{r'\partial\theta'},$$

$$Q'_{z'r'} = \omega'_{3113}\frac{\partial u_{r'}}{\partial z'} + \omega'_{3131}\frac{\partial u_{z'}}{\partial r'}, \quad Q'_{r'z'} = \omega'_{1313}\frac{\partial u_{r'}}{\partial z'} + \omega'_{1331}\frac{\partial u_{z'}}{\partial r'}. \tag{4}$$

In (3) and (4) through $Q'_{r'r'}$, $Q'_{\theta'\theta'}$,..., and $Q'_{r'z'}$, perturbation of the components of the non-symmetric Kirchhoff stress tensor is denoted. The notation $u_{r'}$, $u_{\theta'}$ and $u_{z'}$ shows the perturbation of the components of the displacement vector, where ρ' is the density of the cylinder material in the initial state. The constants ω'_{1111}, ω'_{1122},..., and ω'_{1331} in (4), are determined through the following expressions:

$$\omega'_{1111} = \frac{1}{\lambda_3}(\lambda+2\mu), \quad \omega'_{1122} = \frac{1}{\lambda_3}\lambda, \quad \omega'_{1133} = \frac{1}{\lambda_1}\lambda, \quad \omega'_{1221} = \frac{1}{\lambda_3}\mu,$$

$$\omega'_{1313} = 2\mu(\lambda_1+\lambda_3)^{-1}, \quad \omega'_{1331} = 2\mu(\lambda_1+\lambda_3)^{-1}, \quad \omega'_{3113} = \frac{\lambda_3^2}{\lambda_1^2}2\mu(\lambda_1+\lambda_3)^{-1},$$

$$\omega'_{3333} = \frac{\lambda_3}{\lambda_1^2}(\lambda+2\mu), \quad \omega'_{2222} = \omega'_{1111}, \quad \omega'_{2233} = \omega'_{1133}, \quad \omega'_{2323} = \omega'_{1313},$$

$$\omega'_{2112} = \omega'_{1221}, \quad \omega'_{3223} = \omega'_{3113}, \quad \omega'_{2332} = \omega'_{1331}, \quad \omega'_{1111} - \omega'_{1122} = \omega'_{1221} + \omega'_{1212}. \tag{5}$$

For explanation of the foregoing equations and relations, according to Truestell (1961), Eringen and Suhubi (1975), and Guz (2004), let us consider briefly some basic relationships of the large (finite) elastic deformation theory, and their linearization, which are used in the present investigation.

2.1 Some relations of the non-linear theory of elasticity for hyper-elastic bodies.

Consider the definition of the stress and strain tensors in the large elastic deformation theory. For this purpose we use the Lagrange coordinates r, θ and z in the cylindrical system of coordinates $Or\theta z$. In this case, the physical components of Green's strain tensor $\tilde{\varepsilon}$ in the $Or\theta z$ coordinate system are determined by the physical components u_r, $u_\theta$and u_z of the displacement vector **u** through the relation (A1) given in Appendix A.

Consider the determination of the Kirchhoff stress tensor. The use of various types of stress tensors in the large (finite) elastic deformation theory is connected with the reference of the components of these tensors to the unit area of the relevant surface elements in the deformed or un-deformed state. This is because, in contrast to the

linear theory of elasticity, in the finite elastic deformation theory, the difference between the areas of the surface elements, taken before and after deformation must be accounted for, for the derivation of the equation of motion and under satisfaction of the boundary conditions. According to the aim of the present investigation, here we consider two types of stress tensors denoted by $\tilde{\mathbf{q}}$ and $\tilde{\mathbf{s}}$, the components of which refer to the unit area of the relevant surface elements in the un-deformed state, but which act on the surface elements in the deformed state. The physical components $s_{(ij)}$ of the stress tensor $\tilde{\mathbf{s}}$ are determined through the strain energy potential $\Phi = \Phi(\varepsilon_{rr}, \varepsilon_{\theta\theta}, ..., \varepsilon_{\theta z})$ by use of the following expression:

$$s_{(ij)} = \frac{1}{2}\left(\frac{\partial}{\partial \varepsilon_{(ij)}} + \frac{\partial}{\partial \varepsilon_{(ji)}}\right)\Phi, \tag{6}$$

where $(ij) = rr,\ \theta\theta,\ zz,\ r\theta,\ rz,\ z\theta$.

The physical components of the stress tensor $\tilde{\mathbf{q}}$ are determined through the physical components of the stress tensor $\tilde{\mathbf{s}}$ and the displacement vector $\mathbf{u}$ by the expression (A2) given in Appendix A.

The stress tensor $\tilde{\mathbf{q}}$, whose components are determined by expression (A2), is called the Kirchhoff stress tensor, but the stress tensor $\tilde{\mathbf{s}}$ is called the Lagrange stress tensor. According to the expressions (6) and (A2), the stress tensor $\tilde{\mathbf{s}}$ is symmetric, but the stress tensor $\tilde{\mathbf{q}}$ is non-symmetric. In this case the equation of motion is written as follows:

$$\begin{aligned}
&\frac{\partial q_{rr}}{\partial r} + \frac{\partial q_{\theta r}}{r\partial \theta} + \frac{\partial q_{zr}}{\partial z} + \frac{1}{r}(q_{rr} - q_{\theta\theta}) = \rho \frac{\partial^2 u_r}{\partial t^2},\\
&\frac{\partial q_{r\theta}}{\partial r} + \frac{\partial q_{\theta\theta}}{r\partial \theta} + \frac{1}{r}(q_{r\theta} + q_{\theta r}) + \frac{\partial q_{z\theta}}{\partial z} = \rho \frac{\partial^2 u_\theta}{\partial t^2},\\
&\frac{\partial q_{rz}}{\partial r} + \frac{\partial q_{\theta z}}{r\partial \theta} + \frac{1}{r}q_{rz} + \frac{\partial q_{zz}}{\partial z} = \rho \frac{\partial^2 u_z}{\partial t^2},
\end{aligned} \tag{7}$$

For determination of the stress-strain relations it is necessary to give the explicit expression of the strain energy potential Φ in expression (6). In the present paper, we will use the following expression for the potential Φ which was proposed in a paper by John (1960) and was called the harmonic potential:

$$\Phi = \frac{1}{2}\lambda e_1^2 + \mu e_2, \tag{8}$$

where

$$e_1 = \sqrt{1+2\varepsilon_1} + \sqrt{1+2\varepsilon_2} + \sqrt{1+2\varepsilon_3} - 3,$$

$$e_2 = \left(\sqrt{1+2\varepsilon_1}-1\right)^2 + \left(\sqrt{1+2\varepsilon_2}-1\right)^2 + \left(\sqrt{1+2\varepsilon_3}-1\right)^2. \tag{9}$$

In relations (8) and (9), λ and μ are material constants and ε_i $(i = 1,2,3)$ are the principal values of Green's strain tensor.

This completes our consideration of the definition of the stress and strain tensors, the determination of the relations between them, and the equation of motion in the finite elastic deformation theory.

2.2 Determination of the initial strains and stresses.

Substituting the expression (1) into the relation (A1) and supplying them both with the upper index "0" we obtain the following initial strains:

$$\varepsilon^0_{rr} = \varepsilon^0_{\theta\theta} = \frac{1}{2}\left(\lambda_1^2 - 1\right), \quad \varepsilon^0_{zz} = \frac{1}{2}\left(\lambda_3^2 - 1\right), \quad \varepsilon^0_{r\theta} = \varepsilon^0_{rz} = \varepsilon^0_{\theta z} = 0. \tag{10}$$

It follows from (10) that in the initial state, the principal values of Green's strain tensor ε^0_1, ε^0_2, and ε^0_3 coincide with ε^0_{rr}, $\varepsilon^0_{\theta\theta}$ and ε^0_{zz}, respectively. Consequently, substituting the expression (10) into the relations (8) and (9) we obtain the following expression for the strain energy potential in the initial state:

$$\Phi^0 = \frac{1}{2}\lambda\left(2\lambda_1 + \lambda_3 - 3\right)^2 + \mu\left(2\left(\lambda_1 - 1\right)^2 + \left(\lambda_3 - 1\right)^2\right). \tag{11}$$

According to the expression (10), the following relations can be written:

$$\frac{\partial}{\partial\varepsilon^0_{rr}} = \frac{\partial}{\partial\varepsilon^0_{\theta\theta}} = \frac{1}{\lambda_1}\frac{\partial}{\partial\lambda_1}, \quad \frac{\partial}{\partial\varepsilon^0_{zz}} = \frac{1}{\lambda_3}\frac{\partial}{\partial\lambda_3}. \tag{12}$$

Using (11) and (12) we obtain the following expressions for the stresses in the initial state:

$$s^0_{zz} = \left[\lambda\left(2\lambda_1 + \lambda_3 - 3\right) + 2\mu\left(\lambda_3 - 1\right)\right]\left(\lambda_3\right)^{-1}, \quad s^0_{r\theta} = s^0_{rz} = s^0_{z\theta} = 0,$$

$$s^0_{rr} = s^0_{\theta\theta} = \left[\lambda\left(2\lambda_1 + \lambda_3 - 3\right) + 2\mu\left(\lambda_1 - 1\right)\right]\left(\lambda_1\right)^{-1}. \tag{13}$$

According to the problem statement, we can write that:

$$s^0_{rr} = s^0_{\theta\theta} = \left[\lambda\left(2\lambda_1 + \lambda_3 - 3\right) + 2\mu\left(\lambda_1 - 1\right)\right]\left(\lambda_1\right)^{-1} = 0,$$

and from this we obtain:

$$\lambda_1 = \left[2 - \frac{\lambda}{\mu}\left(\lambda_3 - 3\right)\right]\left[2\left(\frac{\lambda}{\mu} + 1\right)\right]^{-1}. \tag{14}$$

Also, we obtain from (13), (1) and (A2) the following expressions for the Kirchhoff stress tensor in the initial state:

$$q^0_{zz} = \lambda_3 s^0_{zz}, \quad q^0_{rr} = \lambda_1 s^0_{rr} = 0, \quad q^0_{\theta\theta} = \lambda_1 s^0_{\theta\theta} = 0,$$

$$q^0_{\theta r} = q^0_{r\theta} = q^0_{rz} = q^0_{zr} = q^0_{z\theta} = q^0_{\theta z} = 0. \tag{15}$$

It follows from the relations (1) and (15) that the equation (7) satisfies automatically the initial strain-stress state.

2.3 Determination of the relations related to the perturbation state.

Now we assume that the considered cylinders with the foregoing initial strain-stress state has an additional small perturbation determined by the displacement vector with components $u^{(k)}_r = u^{(k)}_r(r,\theta,z,t)$, $u^{(k)}_\theta = u^{(k)}_\theta(r,\theta,z,t)$ and $u^{(k)}_z = u^{(k)}_z(r,\theta,z,t)$. Taking into account the smallness of the displacement perturbation, we linearize the relationships (A1), (6), (A2) and (7) – (9) for the perturbed state in the vicinity of the appropriate values for the initial state and then subtract from them the relationships for the initial state. As a result, we obtain the equations of the TLTEWISB. As an example, in the case under consideration, as a result of the aforementioned linearization we obtain the following expressions for perturbation of the components of Green's strain tensor:

$$\varepsilon_{rr} = \lambda_1 \frac{\partial u_r}{\partial r}, \quad \varepsilon_{r\theta} = \lambda_1 \frac{1}{2}\left(\frac{\partial u_\theta}{\partial r} + \frac{\partial u_r}{r\partial\theta} - \frac{u_\theta}{r}\right), \quad \varepsilon_{rz} = \frac{1}{2}\left(\lambda_1 \frac{\partial u_r}{\partial z} + \lambda_3 \frac{\partial u_z}{\partial r}\right),$$

$$\varepsilon_{\theta\theta} = \lambda_1 \frac{1}{2}\left(\frac{\partial u_\theta}{r\partial\theta} + \frac{u_r}{r}\right), \quad \varepsilon_{rz} = \frac{1}{2}\left(\lambda_3 \frac{\partial u_z}{r\partial\theta} + \lambda_1 \frac{\partial u_\theta}{\partial z}\right), \quad \varepsilon_{zz} = \lambda_3 \frac{\partial u_z}{\partial z}. \tag{16}$$

Perturbation of the components of the stress tensor $\tilde{\mathbf{s}}$ (denoted by capital letter $S_{(ij)}$, where $(ij) = rr,\ \theta\theta,\ zz,\ r\theta,\ rz,\ z\theta$) is determined from linearization of the relations (6), (8) and (9). We do not consider this linearization procedure in detail here, but note that as a result of this linearization the following expressions for $S_{(ij)}$ are obtained:

$$S_{rr} = \lambda\varepsilon + 2\mu\varepsilon_{rr}, \quad S_{\theta\theta} = \lambda\varepsilon + 2\mu\varepsilon_{\theta\theta}, \quad S_{zz} = \lambda\varepsilon + 2\mu\varepsilon_{zz}, \quad \varepsilon = \varepsilon_{rr} + \varepsilon_{\theta\theta} + \varepsilon_{zz},$$

$$S_{r\theta} = 2\mu\varepsilon_{r\theta}, \quad S_{rz} = 2\mu\varepsilon_{rz}, \quad S_{z\theta} = 2\mu\varepsilon_{z\theta}. \tag{17}$$

Taking into account the relation (17), we obtain from (A2) (given in Appendix A) the following expression for perturbation of the components of the Kirchhoff stress tensor $\tilde{\mathbf{q}}$ (denoted by capital letter $Q_{(ij)}$).

$$Q_{rr} = \lambda_1 S_{rr}, \quad Q_{r\theta} = \lambda_1 S_{r\theta}, \quad Q_{rz} = \lambda_3 S_{rz}, \quad Q_{\theta r} = \lambda_1 S_{r\theta}, \quad Q_{\theta\theta} = \lambda_1 S_{\theta\theta},$$

$$Q_{zr} = \lambda_1 S_{zr} + S^0_{zz}\frac{\partial u_r}{\partial z}, \quad Q_{z\theta} = \lambda_1 S_{z\theta} + S^0_{zz}\frac{\partial u_\theta}{\partial z}, \quad Q_{zz} = \lambda_3 S_{zz}. \tag{18}$$

Substituting $(q^0_{(ij)} + Q_{(ij)})$ and $(u^0_{(i)} + u_{(i)})$ (where $(i) = r, \theta, z$) instead of $q_{(ij)}$ and $u_{(i)}$, respectively in Eq. (7) we obtain:

$$\frac{\partial Q_{rr}}{\partial r} + \frac{\partial Q_{\theta r}}{r\partial\theta} + \frac{\partial Q_{zr}}{\partial z} + \frac{1}{r}(Q_{rr} - Q_{\theta\theta}) = \rho\frac{\partial^2 u_r}{\partial t^2},$$

$$\frac{\partial Q_{r\theta}}{\partial r} + \frac{\partial Q_{\theta\theta}}{r\partial\theta} + \frac{1}{r}(Q_{r\theta} + Q_{\theta r}) + \frac{\partial Q_{z\theta}}{\partial z} = \rho\frac{\partial^2 u_\theta}{\partial t^2},$$

$$\frac{\partial Q_{rz}}{\partial r} + \frac{\partial Q_{\theta z}}{r\partial\theta} + \frac{1}{r}Q_{rz} + \frac{\partial Q_{zz}}{\partial z} = \rho\frac{\partial^2 u_z}{\partial t^2}. \tag{19}$$

Multiplying Eq. (19) by $(\lambda_1^2\lambda_3)^{-1}$ and using the notation

$$\rho' = (\lambda_1^2\lambda_3)^{-1}\rho, \quad r' = \lambda_1 r, \quad z' = \lambda_3 z, \quad Q'_{r'r'} = (\lambda_1\lambda_3)^{-1}Q_{rr}, \quad Q'_{z'z'} = (\lambda_1^2)^{-1}Q_{zz},$$

$$Q'_{\theta'\theta'} = (\lambda_1\lambda_3)^{-1}Q_{\theta\theta}, \quad Q'_{r'\theta'} = (\lambda_1\lambda_3)^{-1}Q_{r\theta}, \quad Q'_{\theta'r'} = (\lambda_1\lambda_3)^{-1}Q_{\theta r},$$

$$Q'_{z'\theta'} = (\lambda_1^2)^{-1}Q_{z\theta},\ Q'_{\theta'z'} = (\lambda_1\lambda_3)^{-1}Q_{\theta z},\ Q'_{r'z'} = (\lambda_1\lambda_3)^{-1}Q_{rz},\ Q'_{z'r'} = (\lambda_1\lambda_3)^{-1}Q_{zr} \tag{20}$$

we obtain Eq. (3) from Eq. (19). Moreover, from the relationships (17), (18) and (20) we derive the expressions in (5) for ω'_{1111}, ω'_{1122},..., and ω'_{1331} which enter the elasticity relations (4).

Now we formulate the boundary conditions. These conditions are:

for the solid cylinder

$$Q'_{r'r'}\big|_{r'=\lambda_1 R} = 0, \quad Q'_{r'\theta'}\big|_{r'=\lambda_1 R} = 0, \quad Q'_{r'z'}\big|_{r'=\lambda_1 R} = 0. \tag{21}$$

for the hollow cylinder

$$Q'_{r'r'}\big|_{r'=\lambda_1 R} = 0, \quad Q'_{r'\theta'}\big|_{r'=\lambda_1 R} = 0, \quad Q'_{r'z'}\big|_{r'=\lambda_1 R} = 0,$$

$$Q'_{r'r'}\big|_{r'=\lambda_1 (R-h)} = 0, \quad Q'_{r'\theta'}\big|_{r'=\lambda_1 (R-h)} = 0, \quad Q'_{r'z'}\big|_{r'=\lambda_1 (R-h)} = 0. \tag{22}$$

This completes formulation of the problems and consideration of the related equations and relationships.

3 Solution procedure and obtaining the dispersion equation

For solution of the eigenvalue problems (3) – (5), (21) and (22) we use the representation:

$$u_{r'} = \frac{1}{r'}\frac{\partial}{\partial\theta'}\Psi - \frac{\partial^2}{\partial r'\partial z'}\mathrm{X}, \quad u_{\theta'} = -\frac{\partial}{\partial r'}\Psi - \frac{1}{r'}\frac{\partial^2}{\partial\theta'\partial z'}\mathrm{X},$$

$$u_{z'} = (\omega'_{1133}+\omega'_{1313})^{-1}\left(\omega'_{1111}\Delta'_1 + \omega'_{3113}\frac{\partial^2}{\partial z'^2} - \rho'\frac{\partial^2}{\partial t^2}\right)\mathrm{X},$$

$$\Delta'_1 = \frac{\partial^2}{\partial r'^2} + \frac{1}{r'}\frac{\partial}{\partial r'} + \frac{1}{r'^2}\frac{\partial^2}{\partial\theta'^2}, \tag{23}$$

which is proposed by Guz (1986a, 2004). Here the functions Ψand X are the solutions of the equations

$$\left(\Delta'_1 + \xi'^2_1\frac{\partial^2}{\partial z'^2} - \frac{\rho'}{\omega'_{1221}}\frac{\partial^2}{\partial t^2}\right)\Psi = 0, \quad \left[\left(\Delta'_1 + \xi'^2_2\frac{\partial^2}{\partial z'^2}\right)\left(\Delta'_1 + \xi'^2_3\frac{\partial^2}{\partial z'^2}\right) + \right.$$

$$\left. -\rho'\left(\frac{\omega'_{1111}+\omega'_{1331}}{\omega'_{1111}\omega'_{1331}}\Delta'_1 + \frac{\omega'_{3333}+\omega'_{3113}}{\omega'_{1111}\omega'_{1331}}\frac{\partial^2}{\partial z'^2}\right)\frac{\partial^2}{\partial t^2} + \frac{\rho'^2}{\omega'_{1111}\omega'_{1331}}\frac{\partial^4}{\partial t^4}\right]\mathrm{X} = 0, \tag{24}$$

where

$$\xi'^2_1 = \omega'_{3113}\left(\omega'_{1221}\right)^{-1}, \quad \xi'^2_2 = c' + \left[c'^2 - \omega'_{3333}\omega'_{3113}\left(\omega'_{1111}\omega'_{1331}\right)^{-1}\right]^{\frac{1}{2}},$$

$$\xi'^2_3 = c' - \left[c'^2 - \omega'_{3333}\omega'_{3113}\left(\omega'_{1111}\omega'_{1331}\right)^{-1}\right]^{\frac{1}{2}},$$

$$c' = \left(2\omega'_{1111}\omega'_{1331}\right)^{-1}\left[\omega'_{1111}\omega'_{3333} + \omega'_{1331}\omega'_{3113} - \left(\omega'_{1133}+\omega'_{1313}\right)^2\right]. \tag{25}$$

For the flexural waves we represent the functions Ψ and X as follows:

$$\Psi = \Psi_n(r')\sin n\theta'\sin(kz'-\omega t), \quad \mathrm{X} = \mathrm{X}_n(r')\cos n\theta'\cos(kz'-\omega t). \tag{26}$$

Substituting the expressions (26) into the equations (24) we obtain

$$\left(\Delta'_{1n} + \zeta'^2_1\right)\Psi_n = 0, \quad \left(\Delta'_{1n} + \zeta'^2_2\right)\left(\Delta'_{1n} + \zeta'^2_3\right)\mathrm{X}_n = 0,$$

$$\Delta'_{1n} = \frac{d^2}{dr'^2} + \frac{d}{r'dr'} - \frac{n^2}{r'^2}, \tag{27}$$

where

$$\zeta'^2_1 = k^2\left(\omega'_{1221}\right)^{-1}\left(\rho' c^2 - \omega'_{3113}\right), \quad c = \frac{k}{\omega} \tag{28}$$

but ζ'^2_2 and ζ'^2_3 are determined as solutions of the equation

$$\omega'_{1111}\omega'_{1331}\zeta'^4 - k^2\zeta'^2\left[\omega'_{1111}\left(\rho' c^2 - \omega'_{3333}\right) + \omega'_{1331}\left(\rho' c^2 - \omega'_{3113}\right) + \left(\omega'_{1133} + \omega'_{1313}\right)^2\right] + k^4\left(\rho' c^2 - \omega'_{3333}\right)\left(\rho' c^2 - \omega'_{3113}\right) = 0. \tag{29}$$

In (28) and (29), c is the phase velocity of the flexural waves.

Thus, we find the solution of the equations in (27) as follows:

for the solid cylinder

$$\Psi_n = A_1 E_n(\zeta'_1 kr'), \quad \mathrm{X}_n = A_2 E_n(\zeta'_2 kr') + A_3 E_n(\zeta'_3 kr'), \tag{30}$$

for the hollow cylinder

$$\Psi_n = A_1 E_n(\zeta'_1 kr') + B_1 D_n(\zeta'_1 kr'), \quad \mathrm{X}_n = A_2 E_n(\zeta'_2 kr') + A_3 E_n(\zeta'_3 kr') + A_2 D_n(\zeta'_2 kr') + A_3 D_n(\zeta'_3 kr'), \tag{31}$$

where

$$E_n(\zeta'_j kr') = J_n(\zeta'_j kr'), \quad D_n(\zeta'_j kr') = Y_n(\zeta'_j kr') \quad if\, \zeta'^2_j > 0,$$

$$E_n(\zeta'_j kr') = I_n(\zeta'_j kr'), \quad D_n(\zeta'_j kr') = K_n(\zeta'_j kr') \quad if\, \zeta'^2_j < 0,$$

$$j = 1,2,3 \tag{32}$$

In (32), $J_n(x)$ and $Y_n(x)$ are Bessel functions of the first and second kind of the $n-th$ order and $I_n(x)$and $K_n(x)$ are Bessel functions of a purely imaginary argument of the $n-th$order and Macdonald functions of the $n-th$order, respectively.

Thus, using equations (30)-(33), (23), (4) and (5) we obtain the dispersion equations from (21) for the solid cylinder and from (22) for the hollow cylinder. This dispersion equation is:

for the solid cylinder

$$\det\left\|\beta^s_{ij}\right\| = 0, \quad i; j = 1,2,3, \tag{33}$$

for the hollow cylinder

$$\det\left\|\beta^h_{ij}\right\| = 0, \quad i; j = 1,2,3,4,5,6. \tag{34}$$

The explicit expressions of β^s_{ij} and β^h_{ij} are given in Appendix B by formulae (B1) and (B2) respectively.

4 Numerical results and discussions

Now we consider the numerical results related to the dispersion curves which are obtained by the numerical solution of the dispersion equations (33) (for the solid cylinder) and (34) (for the hollow cylinder) in the case where $n = 1$in the expressions (30) – (33) and in formulae given in Appendix B. Note that the algorithm of the numerical solution is based on the well-known "bi-section" method. Taking the equation (14) into account, we estimate the magnitude and character of the initial strains through the elongation parameter λ_3 which enters the expressions (1), (2) and (5). Consequently, the results obtained in the cases where $\lambda_3 > 1$ ($\lambda_3 < 1$) will illustrate the influence of the initial stretching (compressing) of the cylinders on the dispersion curves. But the results obtained in the case where $\lambda_3 = 1$ will correspond to the classical ones which were obtained and analyzed in the works by Hudson (1943), Pao and Mindlin (1960), Abramson (1957), Yamakawa and Murakami (1997), Yuan and Hsieh (1998), Ilmenkov and Kleshchev (2012) and others. Note that in obtaining the numerical results, which will be discussed below, it is assumed that $\lambda/\mu = 1.5$.

4.1 Solid cylinder.

First, we analyze the dispersion curves related to the solid cylinder and consider Fig. 2a which shows the dispersion curves related to the first mode. These curves are constructed for various values of the parameter λ_3. The dispersion curve constructed in the case where $\lambda_3 = 1$ coincides with the corresponding one given in the paper by Abramson (1957). It follows from these results that the initial compression of the solid cylinder causes the wave propagation velocity to decrease. In this case the cut-off values of kR(denoted by $(kR)_{cf}$) arise, before which the flexural wave cannot propagate in the cylinder and the values of $(kR)_{cf}$ increase with a decrease in λ_3. The numerical results show that the high wavenumber limit value of the wave propagation velocity, i.e. the limit value of c/c_2 as $kR \to \infty$, is c_R/c_2 where $c_2 = \sqrt{\mu/\rho}$ and $c_R = c_R(\lambda_3)$, is the Rayleigh wave's velocity in the initially stressed half-plane, the material of which coincides with the cylinder's material. Note that the values of $c_R(\lambda_3)$ are determined by the solution of the equation:

$$(\rho' c_R^2 - \omega'_{1221})\omega'_{2112}\left[\omega'_{2222}(\rho' c_R^2 - \omega'_{1111}) + \omega'^2_{1122}\right]^2 -$$

$$\omega'_{2222}(\rho' c_R^2 - \omega'_{1111})\left[\omega'_{2112}(\rho' c_R^2 - \omega'_{1221}) + \omega'^2_{1212}\right]^2 = 0. \tag{35}$$

The low wavenumber limit values of the wave propagation velocity, i.e. the values of c/c_2 as $kR \to (kR)_{cf}$, are almost zero.

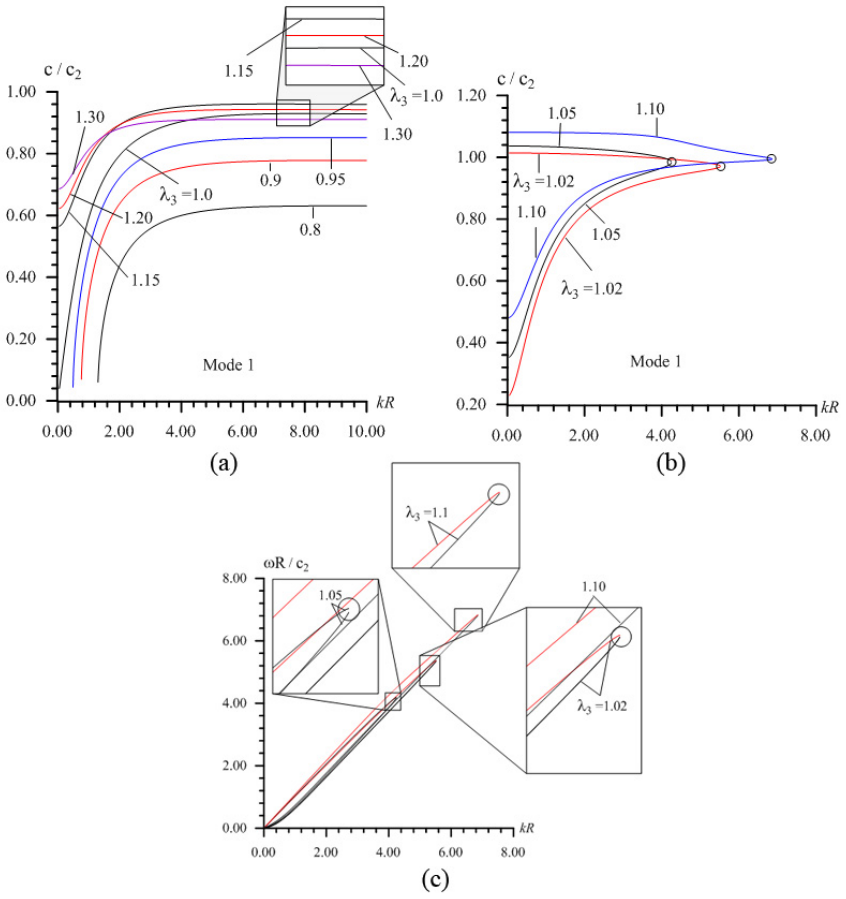

Figure 2: Dispersion curves related to the mode 1 in the cases where (a) $0.8 \leq \lambda_3 \leq 1.0$and $1.15 \leq \lambda_3 \leq 1.3$; (b) $1.02 \leq \lambda_3 \leq 1.1$, as well as dispersion diagrams (c) related to the cases where $1.02 \leq \lambda_3 \leq 1.1$. Solid cylinder

The behavior of the dispersion curves obtained under initial tension is more complicated than those obtained under initial compression of the cylinder. The dispersion curves related to the initially tensioned cylinder in the cases where $1.02 \leq \lambda_3 \leq 1.10$ are given in Fig. 2b, but the dispersion curves related to the cases where $1.15 \leq \lambda_3 \leq 1.30$ are given in Fig. 2a. It follows from Fig. 2b that in the cases where $1.02 \leq \lambda_3 \leq 1.10$, the behavior of the dispersion curves of mode 1 is unusual. So, in these dispersion curves there are points (indicated by circles in Fig. 2b) at which $dc/d(kR) = \infty$. Using the group velocity definition $c_g = d\omega/dk$ and the expression

$k = \omega/c$ we can make the following mathematical manipulations:

$$c_g = \frac{d\omega}{dk} = \frac{d\omega}{d(\omega/c)} = \frac{c^2 d\omega}{cd\omega - \omega dc} = \frac{c^2 d\omega/dk}{cd\omega/dk - \omega R dc/d(kR)} = \frac{c^2 c_g}{cc_g - \omega R dc/d(kR)} \tag{36}$$

We obtain

$$c_g(cc_g - \omega R\frac{dc}{d(kR)} - c^2) = 0 \tag{37}$$

from (36). According to equation (37), we can conclude that at the points for which $dc/d(kR) \quad = \infty$, the solution of the equation (37), which has a real physical meaning, is $c_g = 0$. Consequently, at the points for which $dc/d(kR) = \infty$ and in the narrow vicinity of these points, the stop band zones arise. At the same time, the dependence between kR(denoted by $(kR)_*$) at which $c_g = 0$, and λ_3, is non-monotonic. For example, we obtain: $(kR)_*$= 5.16, 4.66, 4.34, 4.25, 4.32, 4.55 and 6.66 for λ_3= 1.02, 1.03, 1.03, 1.04, 1.05, 1.06, 1.07 and 1.1, respectively.

Note that, according to Fig. 2b, we can conclude that both (upper and lower) branches of the dispersion curves obtained for the same value of λ_3, seem to be connected at the points $kR = (kR)_*$. The wave propagation velocities of these branches approach each other as $kR \to (kR)_*$ and these branches may have a different character in the near vicinity of the stop band zones. For explanation of these characters we consider the dispersion diagrams given in Fig. 2c which correspond to the dispersion curves illustrated in Fig. 2b and recall that if $c > c_g$, the dispersion is considered normal, but if $c < c_g$, it is an anomalous dispersion. Moreover, sometimes there exist cases where $c_g < 0$ and their related waves are called backward waves. The existence and the experimental observation of the backward waves in cylinders and plates were considered in papers by Meitzler (1965), Wolf et al (1988), Lui et al (2000), Werby and Überall (2002), Martson (2003) and others.

It should be noted that the aforementioned normal and anomalous dispersions, as well as the existence of the backward waves can be easily determined by observation of the dispersion diagrams, i.e. the graphs of the dependence between $\omega R/c_2$ and kR. If this diagram has a part which is similar to that shown in Fig. 3a (Fig. 3b) then this part corresponds to the normal (anomalous) dispersion. Moreover, if the dispersion diagram contains a part which is similar to that shown in Fig. 3c or 3d, then the range of the frequency corresponding to this part causes the backward waves to appear.

Consequently, according to the foregoing definitions and the dispersion diagrams given in Fig. 2c which correspond to the dispersion curves given in Fig. 2b, we can conclude that the dispersion related to the lower branch of the dispersion curve

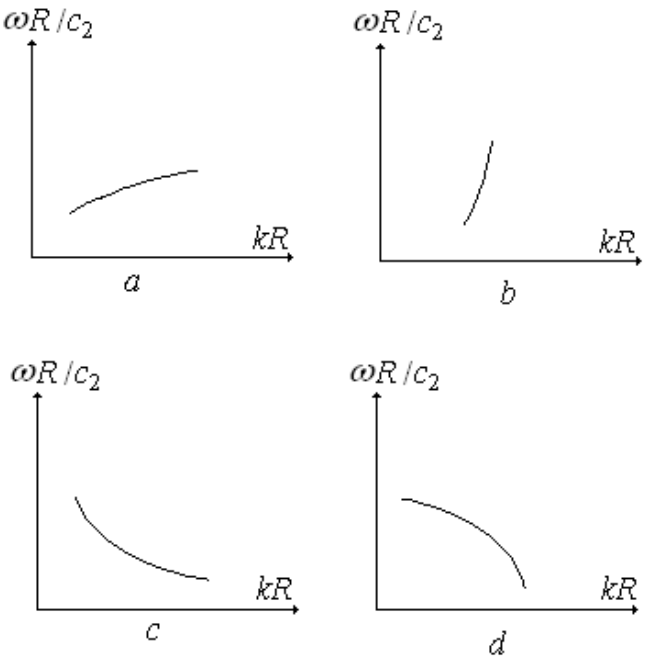

Figure 3: The form of the dispersion diagrams related to the (a) normal, (b) anomalous, (c) and (d) backward waves

in the very near vicinity of the stop band zones can be taken as an anomalous one. But in the remaining part of the dispersion curves given in Fig. 2b, it corresponds to a normal dispersion.

We recall that the results given in Figs. 2b and 2c relate to the cases where $1.02 \leq \lambda_3 \leq 1.10$. But the results obtained for the cases where $\lambda_3 \geq 1.15$, namely for the cases where $1.15 \leq \lambda_3 \leq 1.30$ are given in Fig. 2a. It follows from the dispersion curves given in Fig. 2a, which are related to the latter cases, that before a certain value of kR(denoted by $(kR)'$) an increase in the magnitude of the initial stretching, i.e. an increase in the values of the parameter λ_3, causes the wave propagation velocity to increase. But in the cases where $kR > (kR)'$, the opposite is true; the wave propagation velocity decreases with λ_3 in the range kR as shown in Fig. 2b.

Also, the results illustrated in Figs. 2a and 2b show that the low wavenumber limit values of c/c_2 increase monotonically with λ_3.

Now we analyze the dispersion curves related to the second mode. The numerical results show that the character of these curves depends significantly on the values

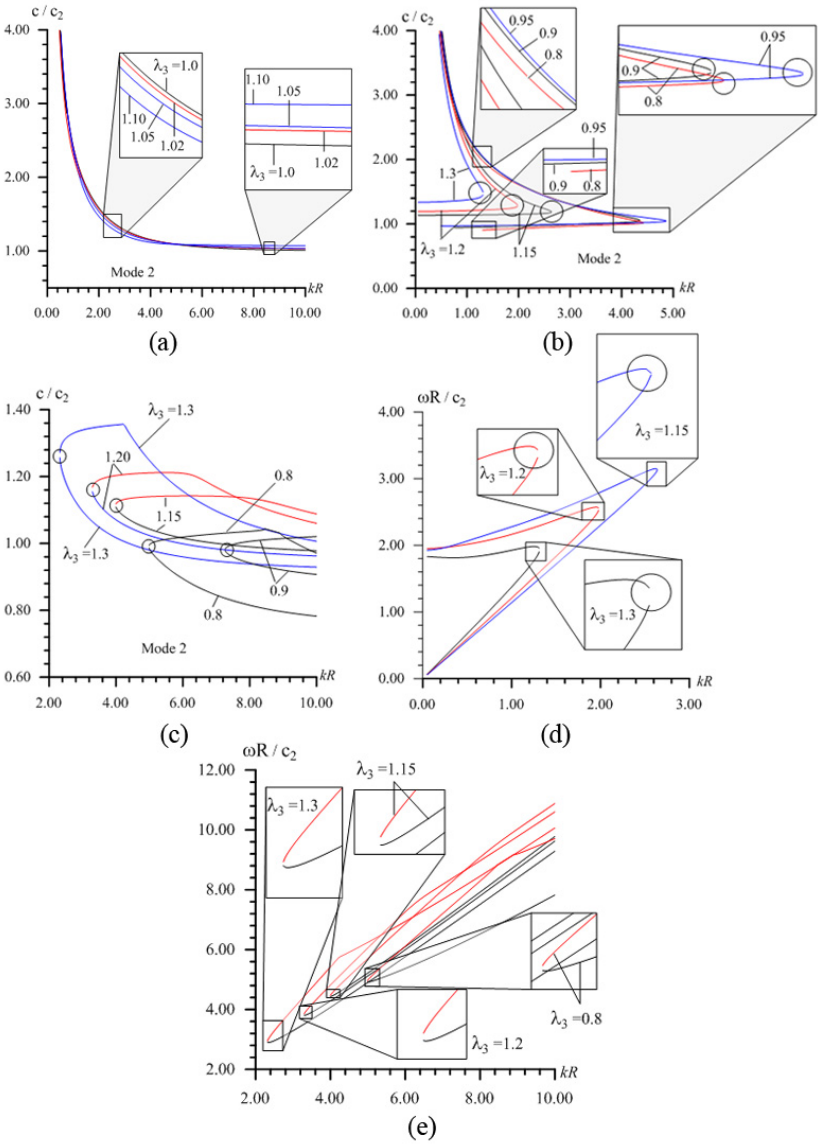

Figure 4: Dispersion curves related to the mode 2 in the cases where (a) $1.02 \leq \lambda_3 \leq 1.1$, (b) $0.8 \leq \lambda_3 \leq 0.95$ and $\lambda_3 = 1.15$, 1.2 and 1.3 (for the first group ones), (c) $\lambda_3 = 0.8$, 0.9, 1.15, 1.20 and 1.4 (for the second group ones); (d) and (e) show dispersion diagrams related to the cases where $\lambda_3 = 1.15$, 1.2 and 1.3 for the first and second group ones respectively. Solid cylinder

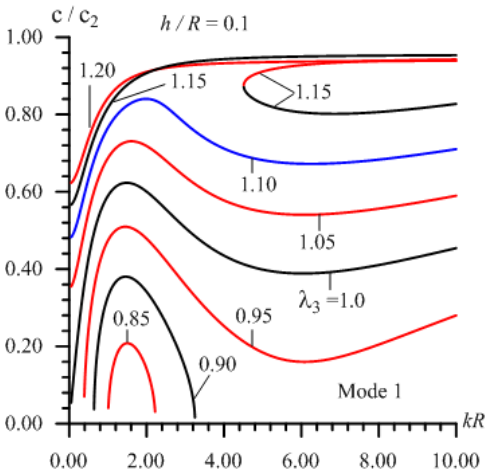

Figure 5: Dispersion curves related to the first mode in the cases where $0.85 \leq \lambda_3 \leq 1.2$ for $h/R = 0.1$. Hollow cylinder

of the parameter λ_3, i.e. on the initial strains in the cylinder. For example, in the cases where $1.0 < \lambda_3 \leq 1.10$ the behavior of the dispersion curves which are illustrated in Fig. 4a, is similar to that which is obtained in the classical case, i.e. in the case where $\lambda_3 = 1.0$. Moreover, Fig. 4a shows that before a certain value of kR (denoted by $(kR)^*_{II}$) an increase in the values of λ_3 causes to decrease, but after this value, i.e. for $kR > (kR)^*_{II}$, increase in the values of the wave propagation velocity c/c_2. Consequently, in the above-noted cases, the influence of the initial tension of the cylinder on the dispersion curves and on the wave propagation velocity is quantitative only. However, a further increase in the values of the parameter λ_3, as well as a further decrease in the values of this parameter (under $\lambda_3 < 1.0$) complicates the character of the dispersion curves. As an example of the influence of the further increase and decrease of λ_3 on the character of the dispersion curves, we consider the cases $1.15 \leq \lambda_3 \leq 1.3$ and $0.80 \leq \lambda_3 \leq 0.95$. The numerical results show that the dispersion curves which relate to these cases are divided into two separate groups. The dispersion curves related to the first (second) group are given in Fig. 4b (Fig. 4c), but the dispersion diagrams for the first (second) group are given in Fig. 4d (Fig. 4e). It follows from these results that each of these dispersion curves has a narrow stop band zone in the near vicinity of the point at which $dc/d(kR) = \infty$ (or $c_g = 0$). In these figures the points are indicated with circles and a zoom into these circles shows that each of the dispersion curves and each of the dispersion diagrams, has two separate branches. Let us call these branches the upper and lower ones.

It follows from Fig. 3 and Fig. 4d that in the near vicinity of the stop band zone the upper branches of the first group of dispersion curves relate to the backward waves, but the lower branches relate to the anomalous dispersion. Also, it follows from Fig. 3 and Fig. 4e that in the near vicinity of the stop band zone the lower branches of the second group of dispersion curves relate to the backward waves, but the upper branches relate to the anomalous dispersion.

According to Fig. 4b, we can conclude that if $1.15 \leq \lambda_3 \leq 1.3$, then the wave propagation velocity related to the upper (lower) branch of the first group of dispersion curves decreases (increases) with λ_3. But in the cases where $0.80 \leq \lambda_3 \leq 0.95$, the wave propagation velocity related to the upper (lower) branch increases (decreases). However, Fig. 4c shows that the influence of the initial strains on the wave propagation velocity related to the second group of dispersion curves has a more complicated character. Yet, according to Fig. 3c, we can conclude that in the cases where $1.15 \leq \lambda_3 \leq 1.3$, the wave propagation velocity related to the second branch of the second group of dispersion curves decreases with λ_3.

This completes the analyses of the numerical results related to the flexural wave propagation in the solid cylinder.

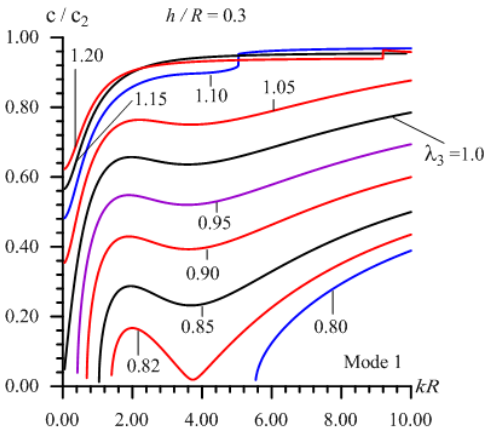

Figure 6: Dispersion curves related to the first mode in the cases where $0.80 \leq \lambda_3 \leq 1.2$ for $h/R = 0.3$. Hollow cylinder

4.2 Hollow cylinder.

Dispersion curves related to the first mode are given in Figs. 5, 6, 7, 8 and 9 for the cases where $h/R = 0.1$, 0.3, 0.5, 0.75 and 0.9, respectively. In these figures the dispersion curves are constructed for various values of the parameter λ_3. Anal-

yses of these results show that under initial compression of the cylinder, i.e. in the cases where $\lambda_3 < 1.0$, there exist cut-off values of kR (denoted by $(kR)^h_{1cf}$) after which the wave propagation takes place. We recall that a similar one has also been established for the dispersion curves of the solid cylinder. However, under flexural wave propagation in the relatively thin hollow cylinder (for example under $h/R < 0.3$) and for the relatively small values of the parameter λ_3 (for example, under $\lambda_3 \leq 0.9$), there is not only $(kR)^h_{1cf}$, but also $(kR)^h_{2cf}$ before which the dispersion curves exist. In other words, the dispersion curves of the first mode exist only in the region $(kR)^h_{1cf} < kR < (kR)^h_{2cf}$. Examples for such dispersion curves are given in Fig. 5 which are depicted for the cases where $\lambda_3 = 0.85$and 0.90. It should be noted that the values of $(kR)^h_{1cf}$ and $(kR)^h_{2cf}$ increase with λ_3.

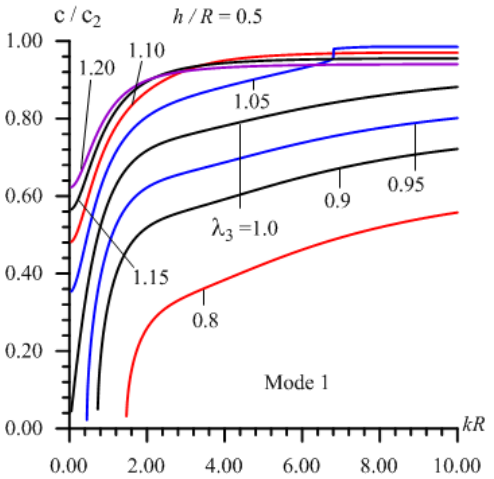

Figure 7: Dispersion curves related to the first mode in the cases where $0.80 \leq \lambda_3 \leq 1.2$ for $h/R = 0.5$. Hollow cylinder

To understand the character of the dispersion curves above, we consider the dispersion diagrams illustrated in Fig. 10. Note that these diagrams correspond to the dispersion curves shown in Fig. 5 and, according to Fig. 3, they confirm that the part of the dispersion curves after the circles constructed for the cases where $\lambda_3 = 0.8$ and 0.9, as well as the part of the dispersion curves between the circles, constructed for the case where $\lambda_3 = 0.95$, relate to the backward waves.

It follows from Figs. 5 – 9 that under initial compression of the cylinder the wave propagation velocity decreases with a decrease in the parameter λ_3. However, under initial tension of the cylinder the influence of this tension on the wave propagation velocity has a complicated character. At the same time, the low wavenumber

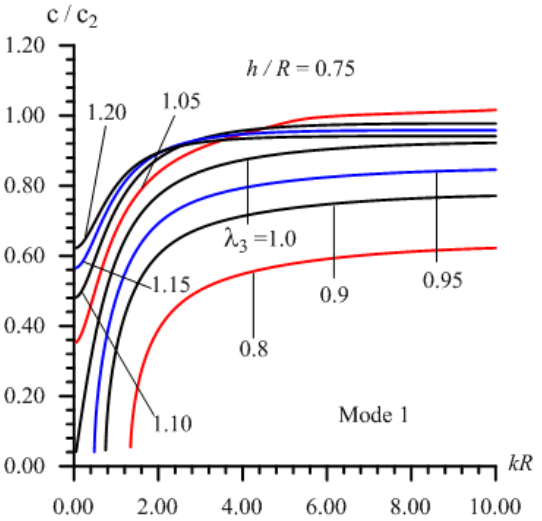

Figure 8: Dispersion curves related to the first mode in the cases where $0.80 \leq \lambda_3 \leq 1.2$ for $h/R = 0.75$. Hollow cylinder

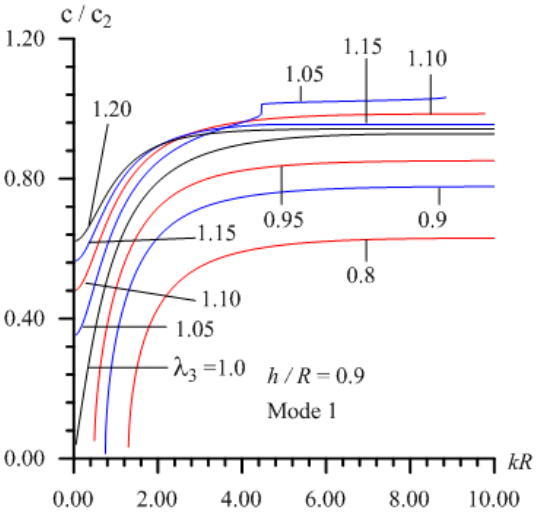

Figure 9: Dispersion curves related to the first mode in the cases where $0.80 \leq \lambda_3 \leq 1.2$ for $h/R = 0.9$. Hollow cylinder

limit values of c/c_2 increase monotonically with λ_3. Moreover, the values of c/c_2 obtained before a certain value of kR also increase with λ_3 when $\lambda_3 > 1.0$.

It should be noted that the high wavenumber limit values of c/c_2 approach (except for the dispersion curves which exist in the finite intervals of kR) $c_R(\lambda_3)/c_2$ as $kR \to \infty$, where $c_R(\lambda_3)$ is determined from the solution of the equation (35).

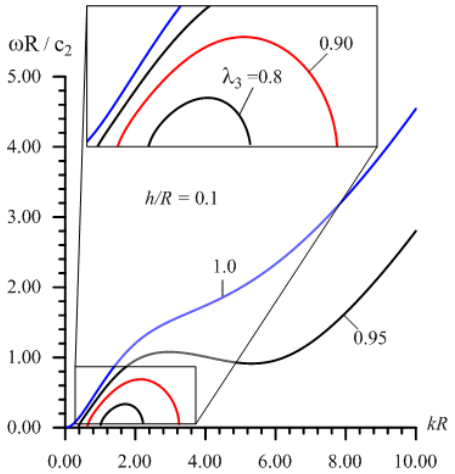

Figure 10: Dispersion diagrams related to the case shown in Fig. 5

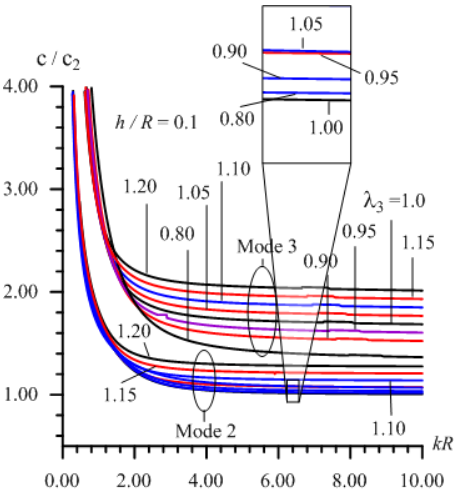

Figure 11: Dispersion curves related to the modes 2 and 3 in the cases where $0.80 \leq \lambda_3 \leq 1.2$ for $h/R = 0.1$. Hollow cylinder

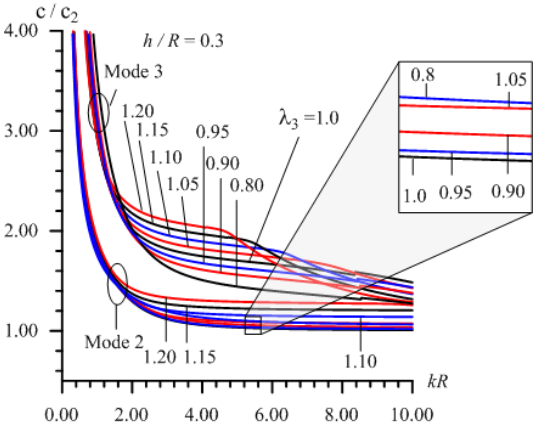

Figure 12: Dispersion curves related to the modes 2 and 3 in the cases where $0.80 \leq \lambda_3 \leq 1.2$ for $h/R = 0.3$. Hollow cylinder

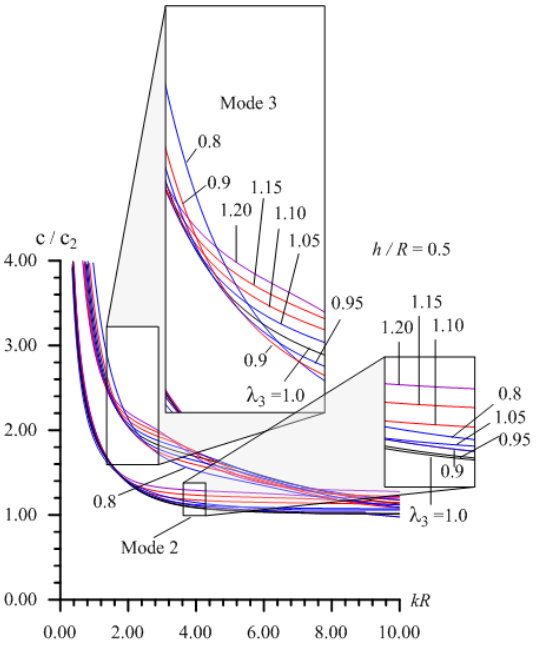

Figure 13: Dispersion curves related to the modes 2 and 3 in the cases where $0.80 \leq \lambda_3 \leq 1.2$ for $h/R = 0.5$. Hollow cylinder

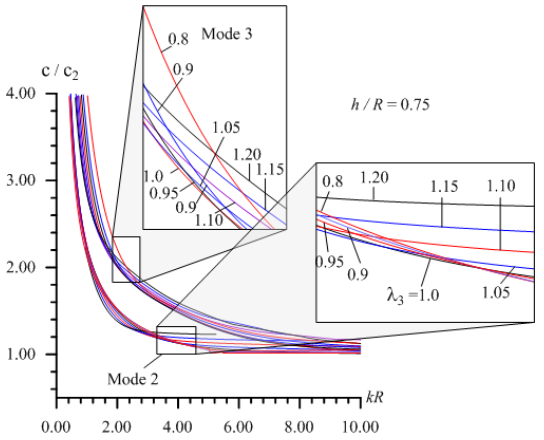

Figure 14: Dispersion curves related to the modes 2 and 3 in the cases where $0.80 \leq \lambda_3 \leq 1.2$ for $h/R = 0.75$. Hollow cylinder

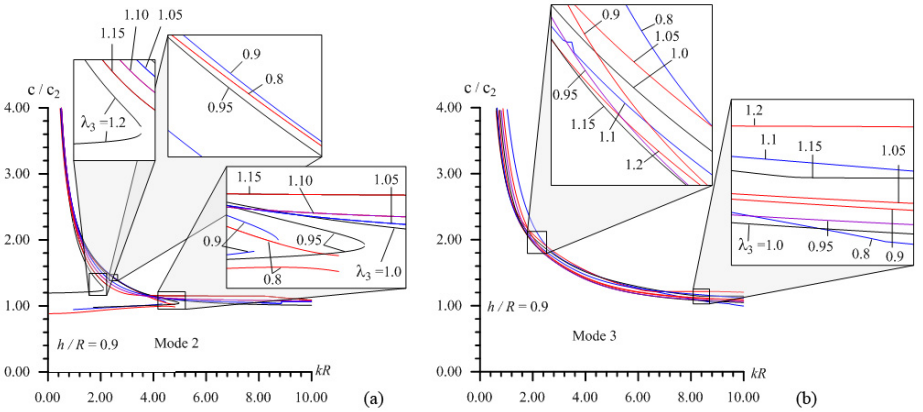

Figure 15: Dispersion curves related to the modes 2 (a) and 3 (b) in the cases where $0.80 \leq \lambda_3 \leq 1.2$ for $h/R = 0.9$. Hollow cylinder

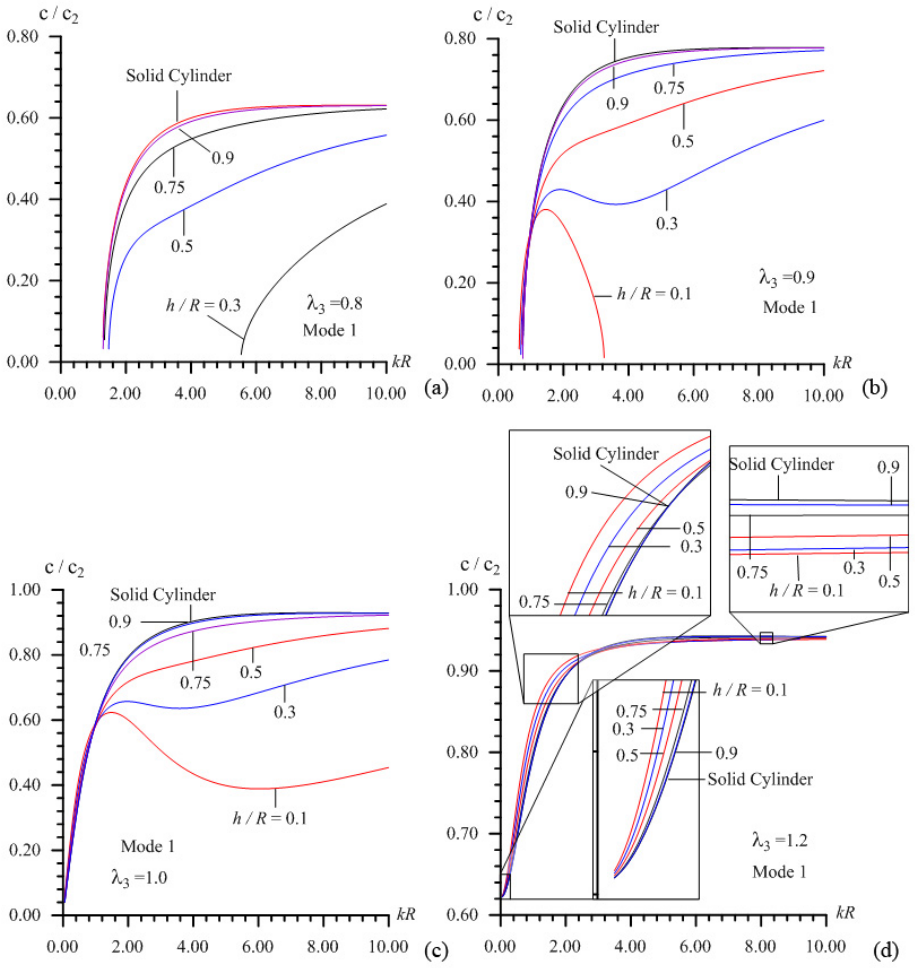

Figure 16: Comparison of the dispersion curves related to the hollow cylinder and obtained for the first mode with the corresponding ones related to the solid cylinder in the cases where λ_3 =0.8 (a), 0.9 (b), 1.0 (c) and 1.2(d)

This completes consideration of the dispersion curves related to the first mode. Now we consider the dispersion curves related to the second and third modes which are given in Figs. 11 – 15 and constructed in the cases where $h/R = 0.1$, 0.3, 0.5, 0.75 and 0.9, respectively. It follows from the analyses of the graphs given in these figures that the character of the influence of the initial strains in the hollow cylinder on the flexural wave propagation velocity depends not only on the values of h/R, but also on the values of the dimensionless wavenumber kR. For example, Fig.

11 shows that in the case where $h/R = 0.1$ for $kR > 0.2$ and in the cases where $\lambda_3 > 1.0$, an increase in the values of λ_3 causes an increase in the values of c/c_2 in the second and third modes. At the same time, a decrease in the values of λ_3 in the cases where $\lambda_3 < 1.0$ causes a decrease in c/c_2. But in mode 2 (mode 3), the values of c/c_2 are greater (less) than the corresponding ones obtained in the case where $\lambda_3 = 1.0$. Observations of Figs. 12, 13 and 14, show that in the cases where $0.3 \leq h/R \leq 0.75$, the dispersion curves (with respect to the influence of the parameter λ_3 on these curves) have almost the same character as those given in Fig. 11. In addition, the character of the dispersion curves obtained in the cases where $h/R = 0.9$ for the third mode and shown in Fig. 15b, is also similar to that of the dispersion curves which are obtained for $h/R \leq 0.75$. However, in the cases where $h/R = 0.9$, the character of the dispersion curves which are obtained for the second mode and shown in Fig. 15a, becomes similar to the character of the dispersion curves which are obtained for the solid cylinder and shown in Fig. 4b. The latter similarity can be explained by the fact that the dispersion curves obtained for the hollow cylinder must approach those obtained for the solid cylinder with h/R. According to this fact, it can be predicted that the dispersion curves obtained for the hollow cylinder in the first mode must also approach the corresponding ones obtained for the solid cylinder with h/R. Note that this prediction is proven with the graphs given in Fig. 16 which are constructed in the cases where $\lambda_3 = 0.8$(Fig. 16a), 0.9 (Fig. 16b), 1.0 (Fig. 16c) and 1.2 (Fig. 16d). Indeed it follows from Fig. 16 that for each selected value of the parameter λ_3, the dispersion curves obtained for the hollow cylinder approach the corresponding ones obtained for the solid cylinder with h/R. Note that these results also prove the validity and reliability of the algorithm and PC programs used in the present investigations.

5 Conclusion

Thus, in the present paper the flexural wave dispersion in the finitely pre-stretched (or pre-compressed) solid and hollow cylinders has been investigated with the use of the TLTEWISB. It is assumed that the initial strains in the cylinders are homogeneous and correspond to the uniaxial tension or compression along their central axes. The elasticity relations of the cylinders' materials are described by the harmonic potential. The analytical solution of the corresponding field equations is presented and, using these solutions, the dispersion equations for the cases under consideration are obtained. The dispersion equations are solved numerically and based on these solutions, the dispersion curves and dispersion diagrams are constructed for various values of the elongation parameter λ_3, through which the magnitude of the initial strains is determined. The curves and diagrams are obtained for the first and second lowest modes of the solid cylinder, and for the first three

lowest modes of the hollow cylinder. Analyses of these numerical results allow us to make the following general conclusions:

- Finite initial uniaxial stretching, as well as finite initial uniaxial compressing, change the dispersion of the flexural waves in the solid and hollow cylinders not only quantitatively, but also qualitatively;
- As a result of the existence of the finite initial strains in the cylinders, parts of the dispersion curves can arise which relate to the backward waves and anomalous dispersion;
- The high wavenumber limit values of the flexural wave propagation velocity in the cylinders in the first mode approach the Rayleigh wave propagation velocity in the corresponding pre-strained half-plane;
- Initial tension of the cylinders causes the low wavenumber limit values of the flexural wave propagation velocity in the first mode to increase;
- Initial compression of the cylinders causes cut-off values of the dimensionless wavenumber in the first mode to appear and these cut-off values increase monotonically with the initial compression;
- Initial compression of the relatively thin hollow cylinder in the first mode causes not only cut-off values of the dimensionless wavenumber to arise, but also causes a value of this wavenumber to appear, after which the flexural wave propagation stops.

Details of the foregoing and many other conclusions are given in the text of the paper.

Appendix A.

First, we write the expression for calculation of the physical components of Green's strain tensor through the physical components of the displacement vector in the cylindrical system of coordinates.

$$\varepsilon_{rr} = \frac{\partial u_r}{\partial r} + \frac{1}{2}\left\{\left(\frac{\partial u_r}{\partial r}\right)^2 + \left(\frac{\partial u_\theta}{\partial r}\right)^2 + \left(\frac{\partial u_z}{\partial r}\right)^2\right\},$$

$$\varepsilon_{r\theta} = \frac{1}{2}\left(\frac{\partial u_\theta}{\partial r} + \frac{\partial u_r}{r\partial\theta} - \frac{u_\theta}{r}\right) + \frac{1}{2}\left\{\frac{\partial u_r}{\partial r}\left(\frac{\partial u_r}{r\partial\theta} - \frac{u_\theta}{r}\right) + \frac{\partial u_\theta}{\partial r}\left(\frac{\partial u_\theta}{r\partial\theta} + \frac{u_r}{r}\right) + \frac{\partial u_z}{\partial r}\frac{\partial u_z}{r\partial\theta}\right\},$$

$$\varepsilon_{rz}=\frac{1}{2}\left(\frac{\partial u_r}{\partial z}+\frac{\partial u_z}{\partial r}\right)+\frac{1}{2}\left\{\frac{\partial u_r}{\partial r}\frac{\partial u_r}{\partial z}+\frac{\partial u_\theta}{\partial r}\frac{\partial u_\theta}{\partial z}+\frac{\partial u_z}{\partial r}\frac{\partial u_z}{\partial z}\right\},$$

$$\varepsilon_{\theta\theta}=\frac{\partial u_\theta}{r\partial\theta}+\frac{u_r}{r}+\frac{1}{2}\left\{\left(\frac{\partial u_r}{r\partial\theta}-\frac{u_\theta}{r}\right)^2+\left(\frac{\partial u_\theta}{r\partial\theta}+\frac{u_r}{r}\right)^2+\frac{1}{r^2}\left(\frac{\partial u_z}{\partial\theta}\right)^2\right\},$$

$$\varepsilon_{\theta z}=\frac{1}{2}\left(\frac{\partial u_z}{r\partial\theta}+\frac{\partial u_\theta}{\partial z}\right)+\frac{1}{2}\left\{\frac{\partial u_r}{\partial z}\left(\frac{\partial u_r}{r\partial\theta}-\frac{u_\theta}{r}\right)+\frac{\partial u_\theta}{\partial z}\left(\frac{\partial u_\theta}{r\partial\theta}+\frac{u_r}{r}\right)+\frac{1}{r}\frac{\partial u_z}{\partial\theta}\frac{\partial u_z}{\partial z}\right\},$$

$$\varepsilon_{zz}=\tfrac{\partial u_z}{\partial z}+\tfrac{1}{2}\left\{\left(\tfrac{\partial u_r}{\partial z}\right)^2+\left(\tfrac{\partial u_\theta}{\partial z}\right)^2+\left(\tfrac{\partial u_z}{\partial z}\right)^2\right\}. \tag{A1}$$

The expressions through which the physical components of the Kirchhoff stress tensor are expressed through the physical components of the Lagrange stress tensor and displacement vector are

$$q_{rr}=s_{rr}(1+\frac{\partial u_r}{\partial r})+s_{r\theta}(\frac{\partial u_r}{r\partial\theta}-\frac{u_\theta}{r})+s_{rz}\frac{\partial u_r}{\partial z},$$

$$q_{r\theta}=s_{rr}\frac{\partial u_\theta}{\partial r}+s_{r\theta}\left(1+\frac{\partial u_\theta}{r\partial\theta}+\frac{u_r}{r}\right)+s_{rz}\frac{\partial u_\theta}{\partial z},$$

$$q_{rz}=s_{rr}\frac{\partial u_z}{\partial r}+s_{r\theta}\frac{\partial u_z}{r\partial\theta}+s_{rz}\left(1+\frac{\partial u_z}{\partial z}\right),$$

$$q_{\theta r}=s_{\theta r}\left(1+\frac{\partial u_r}{\partial r}\right)+s_{\theta\theta}\left(\frac{\partial u_r}{r\partial\theta}-\frac{u_\theta}{r}\right)+s_{\theta z}\frac{\partial u_r}{\partial z},$$

$$q_{\theta\theta}=s_{\theta r}\frac{\partial u_\theta}{\partial r}+s_{\theta\theta}\left(1+\frac{\partial u_\theta}{r\partial\theta}+\frac{u_r}{r}\right)+s_{\theta z}\frac{\partial u_\theta}{\partial z},$$

$$q_{\theta z}=s_{\theta r}\frac{\partial u_z}{\partial r}+s_{\theta\theta}\frac{\partial u_z}{r\partial\theta}+s_{\theta z}\left(1+\frac{\partial u_z}{\partial z}\right),$$

$$q_{zr}=s_{zr}\left(1+\frac{\partial u_r}{\partial r}\right)+s_{z\theta}\left(\frac{\partial u_r}{r\partial\theta}-\frac{u_\theta}{r}\right)+s_{zz}\frac{\partial u_r}{\partial z},$$

$$q_{z\theta}=s_{zr}\frac{\partial u_\theta}{\partial r}+s_{z\theta}\left(1+\frac{\partial u_\theta}{r\partial\theta}+\frac{u_r}{r}\right)+s_{zz}\frac{\partial u_\theta}{\partial z},$$

$$q_{zz}=s_{zr}\tfrac{\partial u_z}{\partial r}+s_{z\theta}\tfrac{\partial u_z}{r\partial\theta}+s_{zz}\left(1+\tfrac{\partial u_z}{\partial z}\right). \tag{A2}$$

Appendix B.

The explicit expressions of $\beta_{ij}^{s}(i;j=1,2,3)$ in the equation (33) are

$$\beta_{11}^{s}=k^{2}\omega_{1111}'\left[\frac{n\zeta_{1}'}{kR'}\,E_{n}'(\zeta_{1}'kR')-\frac{n}{(kR')^{2}}E_{n}(\zeta_{1}'kR')\right]+$$

$$\omega_{1122}'k^{2}\frac{1}{kR'}\left[-n\zeta_{1}'E_{n}'(\zeta_{1}'kR')+\frac{n}{kR'}E_{n}(\zeta_{1}'kR')\right],$$

$$\beta_{12}^{s}=k^{3}\left[\omega_{1111}'\zeta_{2}'^{2}E_{n}''(\zeta_{2}'kR')+\omega_{1122}'\frac{1}{kR'}\left(-\frac{n^{2}}{kR'}E_{n}(\zeta_{2}'kR')+\zeta_{2}'E_{n}'(\zeta_{2}'kR')\right)+\right.$$

$$\left.-\omega_{1133}'\,\frac{\omega_{1111}'d_{2}}{\omega_{1133}'+\omega_{1313}'}E_{n}(\zeta_{2}'kR')\right],$$

$$\beta_{13}^{s}=k^{3}\left[\omega_{1111}'\zeta_{3}'^{2}E_{n}''(\zeta_{3}'kR')+\omega_{1122}'\frac{1}{kR'}\left(-\frac{n^{2}}{kR'}E_{n}(\zeta_{3}'kR')+\zeta_{3}'E_{n}'(\zeta_{3}'kR')\right)+\right.$$

$$\left.-\omega_{1133}'\,\frac{\omega_{1111}'d_{3}}{\omega_{1133}'+\omega_{1313}'}E_{n}(\zeta_{3}'kR')\right],$$

$$\beta_{21}^{s}=k^{2}\left[-\omega_{1221}'\,\zeta_{1}'^{2}E_{n}''(\zeta_{1}'kR')+\omega_{1212}'\left(-\frac{n^{2}}{(kR')^{2}}E_{n}(\zeta_{1}'kR')+\,\frac{\zeta_{1}'}{kR'}E_{n}'(\zeta_{1}'kR')\right)\right],$$

$$\beta_{22}^{s}=k^{3}\left[\omega_{1221}'\left(\frac{n}{(kR')^{2}}E_{n}(\zeta_{2}'kR')-\frac{n\zeta_{2}'}{kR'}E_{n}'(\zeta_{2}'kR')\right)+\right.$$

$$\left.\omega_{1212}'\left(-\frac{n}{kR'}\zeta_{2}'E_{n}'(\zeta_{2}'kR')+\frac{n}{(kR')^{2}}E_{n}(\zeta_{2}'kR')\right)\right],$$

$$\beta_{23}^{s}=k^{3}\left[\omega_{1221}'\left(\frac{n}{(kR')^{2}}E_{n}(\zeta_{3}'kR')-\frac{n\zeta_{3}'}{kR'}E_{n}'(\zeta_{3}'kR')\right)+\right.$$

$$\left.\omega_{1212}'\left(-\frac{n}{kR'}\zeta_{3}'E_{n}'(\zeta_{3}'kR')+\frac{n}{(kR')^{2}}E_{n}(\zeta_{3}'kR')\right)\right],$$

$$\beta_{31}^{s}=k^{2}\omega_{1313}'\frac{n}{kR'}E_{n}(\zeta_{1}'kR'),$$

$$\beta_{32}^{s}=k^{3}\left[\omega_{1313}'\zeta_{2}'E_{n}'(\zeta_{2}'kR')+\omega_{1331}'\,\frac{\omega_{1111}'}{\omega_{1133}'+\omega_{1313}'}\zeta_{2}'d_{2}E_{n}'(\zeta_{2}'kR')\right],$$

$$\beta_{33}^{s}=k^{3}\left[\omega_{1313}'\zeta_{3}'E_{n}'(\zeta_{3}'kR')+\omega_{1331}'\,\frac{\omega_{1111}'}{\omega_{1133}'+\omega_{1313}'}\zeta_{3}'d_{3}E_{n}'(\zeta_{3}'kR')\right]. \tag{B1}$$

The explicit expression of $\beta_{ij}^{h}(i;j=1,2,3,4,5,6)$ in the equation (34) is

$$\beta_{ij}^h = \beta_{ij}^s \text{ for } i;j = 1,2,3,$$

$$\beta_{14}^h = k^2\omega'_{1111}\left[\frac{n\zeta'_1}{kR'}\,D'_n(\zeta'_1kR') - \frac{n}{(kR')^2}D_n(\zeta'_1kR')\right] +$$

$$\omega'_{1122}k^2\frac{1}{kR'}\left[-n\zeta'_1D'_n(\zeta'_1kR') + \frac{n}{kR'}D_n(\zeta'_1kR')\right],$$

$$\beta_{15}^h = k^3\left[\omega'_{1111}\zeta'^2_2D''_n(\zeta'_2kR') + \omega'_{1122}\frac{1}{kR'}\left(-\frac{n^2}{kR'}D_n(\zeta'_2kR') + \zeta'_2D'_n(\zeta'_2kR')\right) +\right.$$

$$\left.-\omega'_{1133}\,\frac{\omega'_{1111}d_2}{\omega'_{1133}+\omega'_{1313}}D_n(\zeta'_2kR')\right],$$

$$\beta_{16}^h = k^3\left[\omega'_{1111}\zeta'^2_3D''_n(\zeta'_3kR') + \omega'_{1122}\frac{1}{kR'}\left(-\frac{n^2}{kR'}D_n(\zeta'_3kR') + \zeta'_3D'_n(\zeta'_3kR')\right) +\right.$$

$$\left.-\omega'_{1133}\,\frac{\omega'_{1111}d_3}{\omega'_{1133}+\omega'_{1313}}D_n(\zeta'_3kR')\right],$$

$$\beta_{24}^h = k^2\left[-\omega'_{1221}\,\zeta'^2_1D''_n(\zeta'_1kR') + \omega'_{1212}\left(-\frac{n^2}{(kR')^2}D_n(\zeta'_1kR') + \frac{\zeta'_1}{kR'}D'_n(\zeta'_1kR')\right)\right],$$

$$\beta_{25}^h = k^3\left[\omega'_{1221}\left(\frac{n}{(kR')^2}D_n(\zeta'_2kR') - \frac{n\zeta'_2}{kR'}D'_n(\zeta'_2kR')\right) +\right.$$

$$\left.\omega'_{1212}\left(-\frac{n}{kR'}\zeta'_2D'_n(\zeta'_2kR') + \frac{n}{(kR')^2}D_n(\zeta'_2kR')\right)\right],$$

$$\beta_{26}^h = k^3\left[\omega'_{1221}\left(\frac{n}{(kR')^2}D_n(\zeta'_3kR') - \frac{n\zeta'_3}{kR'}D'_n(\zeta'_3kR')\right) +\right.$$

$$\left.\omega'_{1212}\left(-\frac{n}{kR'}\zeta'_3D'_n(\zeta'_3kR') + \frac{n}{(kR')^2}D_n(\zeta'_3kR')\right)\right],$$

$$\beta_{34}^h = k^2\omega'_{1313}\frac{n}{kR'}D_n(\zeta'_1kR'),$$

$$\beta_{35}^h = k^3\left[\omega'_{1313}\zeta'_2D'_n(\zeta'_2kR') + \omega'_{1331}\,\frac{\omega'_{1111}}{\omega'_{1133}+\omega'_{1313}}\zeta'_2d_2D'_n(\zeta'_2kR')\right],$$

$$\beta_{36}^h = k^3\left[\omega'_{1313}\zeta'_3D'_n(\zeta'_3kR') + \omega'_{1331}\,\frac{\omega'_{1111}}{\omega'_{1133}+\omega'_{1313}}\zeta'_3d_3D'_n(\zeta'_3kR')\right],$$

$$\beta_{41}^h = k^2\omega'_{1111}\left[\frac{n\zeta'_1}{\chi'}\,E'_n(\zeta'_1\chi') - \frac{n}{(\chi')^2}E_n(\zeta'_1\chi')\right] +$$

$$\omega'_{1122}k^2\frac{1}{\chi'}\left[-n\zeta'_1E'_n(\zeta'_1\chi') + \frac{n}{\chi'}E_n(\zeta'_1\chi')\right],$$

$$\beta^h_{42} = k^3 \left[\omega'_{1111} \zeta'^2_2 E''_n(\zeta'_2\chi') + \omega'_{1122} \frac{1}{\chi'} \left(-\frac{n^2}{\chi'} E_n(\zeta'_2\chi') + \zeta'_2 E'_n(\zeta'_2\chi') \right) + \right.$$
$$\left. -\omega'_{1133} \frac{\omega'_{1111} d_2}{\omega'_{1133} + \omega'_{1313}} E_n(\zeta'_2\chi') \right],$$

$$\beta^h_{43} = k^3 \left[\omega'_{1111} \zeta'^2_3 E''_n(\zeta'_3\chi') + \omega'_{1122} \frac{1}{\chi'} \left(-\frac{n^2}{\chi'} E_n(\zeta'_3\chi') + \zeta'_3 E'_n(\zeta'_3\chi') \right) + \right.$$
$$\left. -\omega'_{1133} \frac{\omega'_{1111} d_3}{\omega'_{1133} + \omega'_{1313}} E_n(\zeta'_3\chi') \right],$$

$$\beta^h_{44} = k^2 \omega'_{1111} \left[\frac{n\zeta'_1}{\chi'} D'_n(\zeta'_1\chi') - \frac{n}{(\chi')^2} D_n(\zeta'_1\chi') \right] +$$
$$\omega'_{1122} k^2 \frac{1}{\chi'} \left[-n\zeta'_1 D'_n(\zeta'_1\chi') + \frac{n}{\chi'} D_n(\zeta'_1\chi') \right],$$

$$\beta^h_{45} = k^3 \left[\omega'_{1111} \zeta'^2_2 D''_n(\zeta'_2 kR') + \omega'_{1122} \frac{1}{\chi'} \left(-\frac{n^2}{\chi'} D_n(\zeta'_2\chi') + \zeta'_2 D'_n(\zeta'_2\chi') \right) + \right.$$
$$\left. -\omega'_{1133} \frac{\omega'_{1111} d_2}{\omega'_{1133} + \omega'_{1313}} D_n(\zeta'_2\chi') \right],$$

$$\beta^h_{46} = k^3 \left[\omega'_{1111} \zeta'^2_3 D''_n(\zeta'_3 kR') + \omega'_{1122} \frac{1}{\chi'} \left(-\frac{n^2}{kR'} D_n(\zeta'_3\chi') + \zeta'_3 D'_n(\zeta'_3\chi') \right) + \right.$$
$$\left. -\omega'_{1133} \frac{\omega'_{1111} d_3}{\omega'_{1133} + \omega'_{1313}} D_n(\zeta'_3\chi') \right],$$

$$\beta^h_{51} = k^2 \left[-\omega'_{1221} \zeta'^2_1 E''_n(\zeta'_1\chi') + \omega'_{1212} \left(-\frac{n^2}{(\chi')^2} E_n(\zeta'_1\chi') + \frac{\zeta'_1}{\chi'} E'_n(\zeta'_1\chi') \right) \right],$$

$$\beta^h_{52} = k^3 \left[\omega'_{1221} \left(\frac{n}{(\chi')^2} E_n(\zeta'_2\chi') - \frac{n\zeta'_2}{\chi'} E'_n(\zeta'_2\chi') \right) + \right.$$
$$\left. \omega'_{1212} \left(-\frac{n}{\chi'} \zeta'_2 E'_n(\zeta'_2\chi') + \frac{n}{(\chi')^2} E_n(\zeta'_2\chi') \right) \right],$$

$$\beta^h_{53} = k^3 \left[\omega'_{1221} \left(\frac{n}{(\chi')^2} E_n(\zeta'_3\chi') - \frac{n\zeta'_3}{\chi'} E'_n(\zeta'_3\chi') \right) + \right.$$
$$\left. \omega'_{1212} \left(-\frac{n}{\chi'} \zeta'_3 E'_n(\zeta'_3\chi') + \frac{n}{(\chi')^2} E_n(\zeta'_3\chi') \right) \right],$$

$$\beta^h_{54} = k^2 \left[-\omega'_{1221} \zeta'^2_1 D''_n(\zeta'_1 kR') + \omega'_{1212} \left(-\frac{n^2}{(kR')^2} D_n(\zeta'_1\chi') + \frac{\zeta'_1}{\chi'} D'_n(\zeta'_1\chi') \right) \right],$$

$$\beta_{55}^h = k^3 \left[\omega'_{1221} \left(\frac{n}{(\chi')^2} D_n(\zeta'_2\chi') - \frac{n\zeta'_2}{\chi'} D'_n(\zeta'_2\chi') \right) + \right.$$

$$\left. \omega'_{1212} \left(-\frac{n}{\chi'} \zeta'_2 D'_n(\zeta'_2\chi') + \frac{n}{(\chi')^2} D_n(\zeta'_2\chi') \right) \right],$$

$$\beta_{56}^h = k^3 \left[\omega'_{1221} \left(\frac{n}{(\chi')^2} D_n(\zeta'_3\chi') - \frac{n\zeta'_3}{\chi'} D'_n(\zeta'_3\chi') \right) + \right.$$

$$\left. \omega'_{1212} \left(-\frac{n}{\chi'} \zeta'_3 D'_n(\zeta'_3\chi') + \frac{n}{(\chi')^2} D_n(\zeta'_3\chi') \right) \right],$$

$$\beta_{61}^h = k^2 \omega'_{1313} \frac{n}{\chi'} E_n(\zeta'_1\chi'),$$

$$\beta_{62}^h = k^3 \left[\omega'_{1313} \zeta'_2 E'_n(\zeta'_2\chi') + \omega'_{1331} \frac{\omega'_{1111}}{\omega'_{1133} + \omega'_{1313}} \zeta'_2 d_2 E'_n(\zeta'_2\chi') \right],$$

$$\beta_{63}^h = k^3 \left[\omega'_{1313} \zeta'_3 E'_n(\zeta'_3\chi') + \omega'_{1331} \frac{\omega'_{1111}}{\omega'_{1133} + \omega'_{1313}} \zeta'_3 d_3 E'_n(\zeta'_3\chi') \right]$$

$$\beta_{36}^h = k^2 \omega'_{1313} \frac{n}{\chi'} D_n(\zeta'_1\chi'),$$

$$\beta_{65}^h = k^3 \left[\omega'_{1313} \zeta'_2 D'_n(\zeta'_2\chi') + \omega'_{1331} \frac{\omega'_{1111}}{\omega'_{1133} + \omega'_{1313}} \zeta'_2 d_2 D'_n(\zeta'_2\chi') \right],$$

$$\beta_{66}^h = k^3 \left[\omega'_{1313} \zeta'_3 D'_n(\zeta'_3\chi') + \omega'_{1331} \frac{\omega'_{1111}}{\omega'_{1133} + \omega'_{1313}} \zeta'_3 d_3 D'_n(\zeta'_3\chi') \right] \quad . \tag{B2}$$

In (B1) and (B2) the following notation is used

$$\chi' = kR'(1 + h/R), \quad R' = \lambda_1 R, \quad E'_n(x) = \frac{dE_n(x)}{dx}, \quad E''_n(x) = \frac{d^2E_n(x)}{dx^2},$$

$$D'_n(x) = \frac{dD_n(x)}{dx}, \quad D''_n(x) = \frac{d^2D_n(x)}{dx^2}, \quad d_2 = -\zeta'^2_2 - \frac{\omega'_{3113}}{\omega'_{1111}} \left(1 - \frac{c^2\mu}{c_{20}^2 \lambda_1^2 \lambda_3 \omega'_{3113}} \right),$$

$$d_3 = -\zeta'^2_3 - \frac{\omega'_{3113}}{\omega'_{1111}} \left(1 - \frac{c^2\mu}{c_{20}^2 \lambda_1^2 \lambda_3 \omega'_{3113}} \right), \quad c_{20}^2 = \sqrt{\mu/\rho}.$$

References

Abramson, H.N. (1957): Flexural waves in elastic beams of circular cross section. *The Journal of the Acoustical Society of America,* vol.29, issue1, pp.42-46.

Akbarov, S.D; Ipek, C.(2010): The influence of the imperfectness of the interface conditions on the dispersion of the axisymmetric longitudinal waves in the pre-strained compound cylinder. *CMES: Computer Modeling in Engineering and Science,* vol.70, no.2, pp.93-121.

Akbarov, S.D.; Ipek, C. (2012): Dispersion of axisymmetric longitudinal waves in a pre-strained imperfectly bonded bi-layered hollow cylinder. *CMC: Computers, Materials, & Continua,* vol.32, no.2, pp.99-144.

Akbarov, S.D.; Guliev, M.S. (2009): Axisymmetric longitudinal wave propagation in a finite pre-strained compound circular cylinder made from compressible materials. *CMES: Computer Modeling in Engineering and Science,* vol. 39, no.2, pp.155–177.

Akbarov, S.D.; Guliev, M.S. (2010): The influence of the finite initial strains on the axisymmetric wave dispersion in a circular cylinder embedded in a compressible elastic medium. *International Journal of Mechanical Sciences,* vol. 52, pp. 89-95.

Akbarov, S.D.; Guliev, M.S.; Tekercioglu, R. (2010): Dispersion relations of the axisymmetric wave propagation in a finite pre-stretched compound circular cylinder made from high elastic incompressible materials. *CMES: Computer Modeling in Engineering and Science,* vol. 55, no. 1, pp. 1–31.

Akbarov, S.D.; Guliev, M.S.; Kepceler, T. (2011). Dispersion relations of axisymmetric wave propagation in initially twisted bi-material compounded cylinders. *Journal of Sound and Vibration*, vol. 330, pp. 1644-1664.

Akbarov, S.D.; Kepceler, T. ; Mert Egilmez, M. (2011): Torsional wave dispersion in a finitely pre-deformed hollow sandwich cylinder. *Journal of Sound and Vibration*, vol. 330, pp. 4519-4537.

Akbarov, S.D.; Kepceler, T. ; Mert Egilmez, M. (2012): On the some particularities of the torsional wave dispersion in a finitely pre-deformed hollow sandwich cylinder. *CMC: Computers, Materials, & Continua,* vol. 30, no.1, pp. 83-98.

Belward, J.A. (1976): The propagation of small amplitude waves in pre-stressed incompressible elastic cylinders. *International Journal of Engineering Science,* vol.14 , issue 8, pp. 647-659.

Biot, M. A., (1965): *Mechanics of Incremental Deformations*, Wiley, New York.

Cooper, R.M.; Naghdi P.M. (1957): Propagation of nonaxially symmetric waves in elastic cylindrical shells. *Journal of the Acoustical Society of America*, vol. 29,

issue 12, pp. 1365-1373.

Eringen, A. C.; Suhubi, E. S. (1975): *Elastodynamics. Vol. I. Finite Motions*, Academic Press, New York, London.

Ilmenkov S.L.; Kleshchev A. A. (2012): The Debye's potentials utilization in the three-dimensional problems of the radiation and propagation of the elastic waves.*International Journal of Theoretical and Mathematical Physics*, vol. 2, issue 6, pp. 163-169

John, F. (1960): Plane strain problems for a perfectly elastic material of harmonic type, *Communications on Pure and Applied Mathematics*, vol. 13, issue 2, pp. 239-296.

Guz, A.N. (1986a): *Elastic Waves in a Body with Initial Stresses I. General Theory,* Kiev, Naukova Dumka, (in Russian).

Guz. A.N. (1986b): *Elastic Waves in a Body with Initial Stresses II. Propagation Laws*, Kiev, Naukova Dumka, 1986 (in Russian).

Guz, A.N. (2004): *Elastic Waves in Bodies with Initial (Residual) Stresses*, Kiev, "A.S.K.", (in Russian).

Guz A.N.; Kushnir V.P.; Makhort F.G. (1975): Flexural waves in solid pre-stressed cylinder. *International Applied Mechanics*, vol. 11, issue 10, pp.1119-1123.

Hudson, G.E. (1943): Dispersion of elastic waves in solid circular cylinders. *Physical Review*, vol. 63, pp. 46-51.

Kepceler, T. (2010): Torsional wave dispersion relations in a pre-stressed bi-material compound cylinder with an imperfect interface. *Applied Mathematical Modelling*, vol. 34, pp. 4058-4073.

Kushnir, V.P. (1983): Numerical study of the laws governing the propagation of bending waves in a hollow compressible cylinder with initial stresses. *Prikladnaya Mekhanica*, vol. 19, issue 12, pp. 113-115 (in Russian).

Lui, T.; Karunasana, W.; Kitipornchai, S.; Veidt, M. (2000): The influence of backward wave transmission on quantitative ultrasonic evaluation using Lamb wave propagation. *Journal of the Acoustical Society of America,* vol. 107, issue 1, pp. 306-314.

Martson, P.L. (2003): Negative group velocity Lamb waves on plates and applications to the scattering of sound by shells. *Journal of the Acoustical Society of America*, vol.113, issue 5, pp. 2659-2662.

Mott, G. (1973): Elastic waveguide propagation in an infinite isotropic solid cylinder that is subjected to a static axial stress and strain. *Journal of the Acoustical Society of America*, vol. 53, pp. 1129-1133.

Meitzler, A.H. (1965): Backward-wave transmission on stress pulses in elastic cylinders and plates. *Journal of the Acoustical Society of America*, vol.38, pp.835-842.

Ozturk, A.; Akbarov, S.D. (2008): Propagation of torsional waves in a pre-stretched compound circular cylinder. *Mechanics of Composite Materials*, vol. 44, issue 1, pp. 77–86.

Ozturk, A.; Akbarov, S.D. (2009a): Torsional wave dispersion relations in a pre-stressed bi-material compounded cylinder. *ZAMM - Journal of Applied Mathematics and Mechanics / Zeitschrift für Angewandte Mathematik und Mechanik*, vol. 89, issue 9, pp. 754–766.

Ozturk, A.; Akbarov, S.D. (2009b): Torsional wave propagation in a pre-stressed circular cylinder embedded in a pre-stressed elastic medium. *Applied Mathematical Modelling*, vol. 33, pp. 3636 - 3649.

Pao Y.H.; Mindlin R.D.(1960): Dispersion of flexural waves in an elastic, circular cylinder. *J. Appl. Mech. Trans. ASME*, vol. 27, pp. 513-520.

Thurston, R.N. (1978): Elastic waves in rods and clad rods. *Journal of the Acoustical Society of America*, vol. 64, issue 1, pp. 1-37.

Truesdell, C. (1961): General and exact theory of waves in finite elastic strain. *Archive for Rational Mechanics and Analyses*, vol. 8, issue 1, pp. 263-296.

Werby, M.F.; Überall, H. (2002): The analysis and interpretation of some special properties of higher order symmetric Lamb waves: The case for plates. *Journal of the Acoustical Society of America*, vol. 111, issue 6, pp. 2686-2691.

Wolf, J.; Ngoc, T.D.K.; Kille, R.; Mayer, W.G. (1988): Investigation of Lamb waves having a negative group velocity. *Journal of the Acoustical Society of America*, vol. 83, issue 1, pp. 122-126.

Yamakawa, J.; Murakami, H. (1997): Longitudinal and flexural wave propagation in reinforced concrete columns. *International Journal of Solids and Structures*, vol. 34 , pp. 4357-4376.

Yuan, F.G.; Hsich, C.C. (1998): Three-dimensional wave propagation in composite cylindrical shells. *Composite Structures*, vol. 42, pp. 153-167.